CHALMERS

Production, Purification and Co-crystallization of *Plasmodium falciparum* and *Plasmodium vivax* Dihydroorotate Dehydrogenase with Novel Inhibitors for Malaria Therapy

LEAH KAGO

Master of Science Thesis in Biotechnology

Department of Chemical and Biological Engineering

CHALMERS UNIVERSITY OF TECHNOLOGY

Göteborg, Sweden 2012.

Production, Purification and Co-crystallization of *Plasmodium falciparum* and *Plasmodium vivax* Dihydroorotate Dehydrogenase with Novel Inhibitors for Malaria Therapy

LEAH KAGO

Department of Chemical and Biological Engineering

CHALMERS UNIVERSITY OF TECHNOLOGY

Göteborg, Sweden 2012.

Production, Purification and Co-crystallization of *Plasmodium falciparum* and *plasmodium vivax* Dihydroorotate Dehydrogenase with Novel inhibitors for Malaria Therapy.

LEAH KAGO

Department of Chemical and Biological Engineering
Chalmers University of Technology
SE-412 96 Göteborg
Sweden
Telephone + 46 (0) 31-772 1000

Production, Purification and Co-crystallization of *Plasmodium falciparum* and *plasmodium vivax* Dihydroorotate Dehydrogenase with Novel inhibitors for Malaria Therapy.

LEAH KAGO

Department of Chemical and Biological Engineering
Chalmers University of Technology

Abstract

Malaria remains a world's disease burden causing high incidences of mortality and morbidity in susceptible populations. Severe cases of malaria mostly caused by parasites of the Apicomplexan *Plasmodium falciparum* are geographically localized in sub-Saharan Africa whereas less severe malaria but the most prevalent outside of Africa; is caused by parasites of *Plasmodium vivax.* A malaria campaign through use of effective drugs such as Artemesins-based-Combination Therapies has considerably reduced mortality cases within the past few years. However, increasing incidences of drug resistance have been reported which raises an urgent need for development of new anti-malaria drugs.

In-silico drug design using the structure of the biological drug target is the latest lead optimization option in search of more potent drugs. In this study, I sought to determine the 3-dimensional structures of *P.falciparum* and *P.vivax* DHODH co-crystallized with novel inhibitors, a putative anti-malaria drug target. For the *P.falciparum* DHODH whose structure is known, the whole process from site directed mutagenesis and classical cloning, protein over- expression, purification to co-crystallization with an inhibitor was performed, for *P.vivax* DHODH with no known resolved structure so far, preliminary protein expression studies and purifications steps were achieved.

*Pf*DHODH was purified to relative purity yielding viable diffracting crystals co-crystallized with an inhibitor whereas the *Pv*DHODH preliminary studies indicated good protein expression profile with need for further optimization in subsequent steps.

Keywords: Malaria, drug resistance, In-silico drug design, DHODH, inhibitors, co-crystallization.

Acknowledgment

The work in this thesis has been accomplished through collective effort and encouragement. I would like to acknowledge the invaluable input, guidance and support from my supervisor, Ass.Prof Rosmarie Friemann throughout the project work at the department of Chemistry and Molecular Biology, Biochemistry and Biophysics, University of Gothenburg. I would also like to acknowledge Prof. Richard Neutze, the Biochemistry and Biophysics leader for the opportunity to work in his group and for examining this thesis work.

I would like to thank project collaborators, Prof. Peter Johnson and Prof. Colin Fishwick, School of Chemistry, University of Leeds for provision of inhibitors and some crystallization conditions.

Special appreciation to my colleagues, Rhawnie Caing-Carlsson for performing initial cloning work, superb orientation to the project and for consistent encouragement, Urszula Eriksson for the insightful advice, Etienne Rebuffet and Anna Frick for screening my crystals at ESRF, Grenoble and the whole Biochemistry group for your assistance in the lab.

I would also like to thank my husband, Francis Kinyanjui for your love and support, my family for moral and financial support during my studies in Sweden and to all my friends for your prayers and encouragement.

Contents

List of abbreviations

ACTs	Artemesinins-based Combination Therapies
DNA	Deoxyribonucleic acid
RNA	Ribonucleic acid
DHODH	Dihydroorotate dehydrogenase
Pf	*Plasmodium falciparum*
Pv	*Plasmodium vivax*
Hs	*Homo sapiens*
IPTG	Isopropyl β-d-1-Thiogalactopyranoside
IMAC	Immobilized Metal Affinity Chromatography
SDS PAGE	Sodium dodecyl sulphate polyacrylamide gel electrophoresis
RBCs	Red blood cells
Ni-NTA	Nickel- Nitriloacetic acid
DTT	Dithiothreitol
TNF-α	Tumor Necrosis factor alpha
IL-12	Interleukin twelve
IFN- γ	Interferon gamma
FMN	Flavin mononucleotide
UV	Ultra violet
PCR	Polymerase chain reaction
dNTPs	Deoxyribonucleotide triphosphates
LB	Luria broth
Rpm	Rotations per minute
HEPES	(4-(2-hydroxyethyl)-1-piperazineethanesulfonic acid)
MWCO	Molecular Weight Cut-Off
CMC	Critical micelle concentration
TEV	Tobacco Etch Virus

1 Introduction

1.1 Project Background

1.1.1 Malaria and Drug Resistance

Malaria is a severe disease burden affecting over 3 billion of the world's population caused by parasites from plasmodium species originating from phylum Apicomplexa and is transmitted by female anopheline mosquitoes. It is endemic in more than 106 countries of the world with over 80% localized in sub-Saharan Africa(*1, 2*). Over 1 million cases of malarial deaths are reported each year with children less than five years of age and pregnant women being most susceptible to the brunt of the disease(*2, 3*).

There are four main human species of plasmodium parasite namely *P.falciparum*, *P.vivax*, *P.ovale*, and *P.malariae*. In the recent past, a fifth human infecting plasmodia species known as *P.knowlesi* originating from monkeys has emerged in South East Asia similar to *P.malariae* but with more severe symptoms(*3, 4*). However, the most severe form of malaria that has caused global concerns and with enormous loss of human life is caused by parasites of *P.falciparum* mostly in endemic African countries. In addition, *P.vivax* localized in Asian countries, parts of Europe and the Americas but quite scarce in Africa; causes some severe clinical symptoms by the fact that the parasites remain dormant in the host system as hypnozoites and can cause relapses after several months or years but it's not as deadly as the *falciparum* strain though affects overall personal health with enormous economic implications(*5, 6*).

Several drugs have been developed over the decades to combat the severity of malaria cases caused by *P.falciparum* and *P.vivax* as well as other less severe strains. Some of the drugs that have been in use include chloroquine, pyrimethamines, sulfonamides as well as the Artemesinins-based Combination Therapies (ACTs). These, coupled with vector control have considerably reduced malarial mortality cases within the last 10 years but cases of drug resistance to most malarial drugs have been reported even with the most effective malarial therapy using ACTs along Thai-Cambodia borderlines(*2, 7*).Therefore, increasing drug resistance against most available drugs including ACTs that have previously been thought to be effective triggers an intense and immediate need for development of new anti-malarial drugs.

The full sequencing of the genomes from *P.falciparum* and *P.vivax* has been helpful in the new phase of drug discovery process in identifying 'druggable' targets i.e. molecules that are able to bind small inhibitor-like molecules with high affinity and selectivity. In particular, the sequencing results from *P.falciparum* indicated absence of genes for salvage pyrimidine biosynthetic pathway but possess only those for *De Novo* pyrimidine biosynthetic pathway(*6, 8*).

There are essentially two ways in which organisms acquire pyrimidines i.e. scavenging preformed pyrimidine bases via salvage pathway or through the *De Novo* pathway that utilizes small molecules to build up larger pyrimidine bases important as building blocks for DNA, RNA, glycoproteins etc (*9*). The parasite thus relies exclusively on the *De Novo* pyrimidine biosynthetic pathway for DNA and RNA formation and hence differs from the human, which utilizes both pathways to replenish these intracellular pools (*8*). This makes the parasite *De Novo* pyrimidine biosynthetic pathway an attractive target for development of new antimalarial drugs since its inhibition would interfere with the parasite proliferation.

1.2 Aim of the Project

The focus of this thesis work was based on Dihydroorotate Dehydrogenase (DHODH), a major and essential *De Novo* pyrimidine biosynthetic pathway enzyme that is a putative drug target. The enzyme is a promising drug target to curb various infectious diseases, among them being the deadly Malaria.

The aim was to elucidate the three dimensional structures of the enzyme DHODH by X-ray diffraction from both *Plasmodium falciparum* and *Plasmodium vivax* species co-crystallized with potent inhibitors developed by project collaborators Prof. Peter Johnson and Prof. Colin Fishwick, School of Chemistry, University of Leeds for structure-based drug design. Using the structure of the biological target, candidate drugs that are predicted to bind with high affinity and selectivity to the target may be designed and re-designed using automated computational procedures.

1.3 Scope of the Project

The project involved *Pf*DHODH and *Pv*DHODH protein expression using constructs codon-optimized for *Escherichia coli* expression system; all protein purifications done by Immobilized Metal Affinity Chromatography (IMAC) and gel filtration chromatography. Co-crystallization of

the biological target with potential inhibitors was set-up by vapour diffusion method and crystals analyzed by X-ray diffraction.

1.4 Background to Methods

1.4.1 Protein Expression system

The *E.coli* expression system is a versatile organism that is mostly used for recombinant protein over-expression and has been widely exploited due to its ease in handling, culturing and fast growth(*10*). The gene of interest can be initially cloned in a vector encoding a polyhistidine tag such that the protein of interest is translated as a fusion protein for ease of purification and identification. In this project, pNIC28-Bsa4 vector (Figure 1), a pET expression vector was used and has a 6xhistidine tag on its N-Terminus fused to a TEV cleavage site peptide. It also has sites for ligation independent cloning (LIC) and *Bsa1* sites important for linearization using *Bsa1* restriction enzyme and *SacB* gene that allow negative selection of the recombinant plasmid in plated agar media supplemented with 5% sucrose. Presence of sucrose clears background colonies from non-recombinant plasmids since *SacB* protein converts them to toxic products and hence they cannot survive on media.

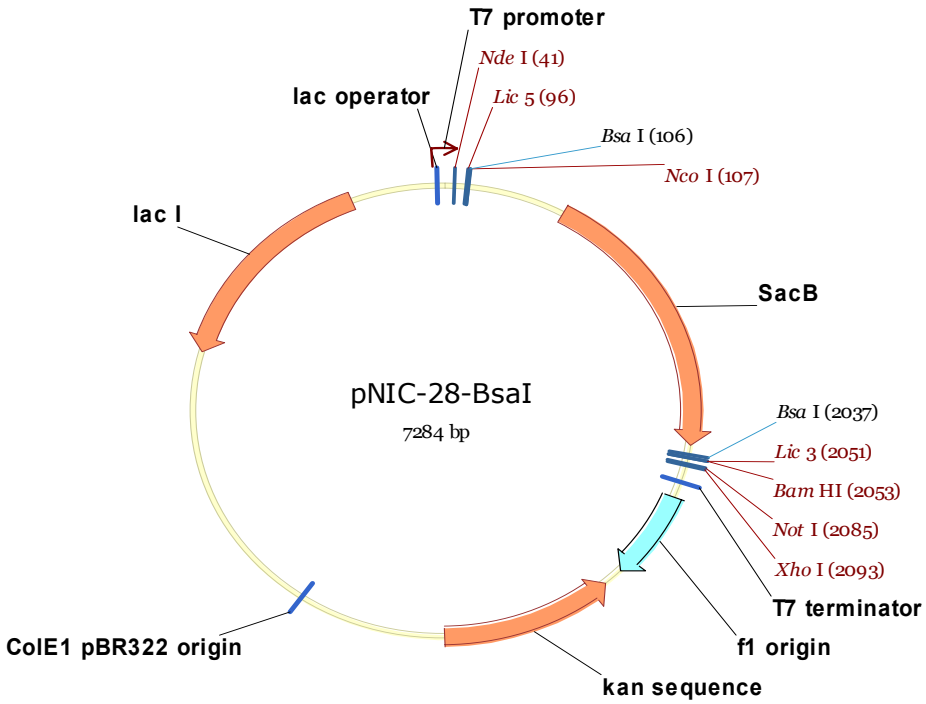

Figure 1: pNIC -28-Bsa4 Vector Map: *Image Source; Structural Genomics Consortium*

The gene of interest is cloned downstream to the T7 promoter in the expression vector i.e. the *SacB* gene is displaced and the gene of interest inserted in its place. T7 promoter system is inducible and specific to T7 RNA polymerase and not the bacterial RNA polymerase. The expression vector once transformed into competent host prokaryotic *E.coli* cells exploits the host lactose operon system. *E.coli* BL21 (DE3) competent cells were used in this project and are known to possess viral derived T7 RNA polymerase, also deficient in *lon* and *omp*T proteases usually present in wild type *E.coli* cells and hence drive over-expression of non-toxic proteins due to their compatibility with T7 promoter system present in most available expression vectors.(*10, 11*)

The lac operator precedes the T7 promoter system and the T7 RNA polymerase can only be activated to initiate transcription of the inserted gene if the lac repressor is displaced from the lac operator. An analogue of lactose, IPTG is capable of displacing the lac repressor and promoting T7 RNA polymerase to initiate transcription of the gene of interest and subsequent protein over-expression at lower induction temperatures(*10*).

1.4.2 Protein Purification

Over-expressed protein of interest is normally purified on basis of its physical and chemical properties. In this project, Fast Performance Liquid Chromatography (FPLC) ÄKTA system was employed to purify the protein of interest with high resolution, purity and stability. Since the protein of interest was over-expressed as a fusion protein with a polyhistidine tag for ease of purification and identification, two purifications methods were used; Immobilized Metal Affinity Chromatography (IMAC) and Molecular Size Exclusion chromatography.

IMAC purification is an affinity chromatography technique that separates tagged proteins by binding reversibly on some insoluble matrix. Histidine tagged proteins react reversibly with immobilized ions on a solid matrix such as Ni-NTA attached to an agarose matrix or Ni^{2+} ions pre-charged on a histrap column and later eluted by changes in pH or competitive elution with different imidazole concentrations.

Molecular Size Exclusion chromatography separates proteins on the basis of size and shape of the molecules. The solid phase usually consists of a column packed with beads of different sizes and separation of protein molecules is based on size of protein molecules and their ability to

transverse through the beads. Therefore, different protein molecules are separated based on their relative molecular masses and eluted as fractions, which can be analyzed by SDS PAGE to identify the protein of interest.(*12*)

1.4.3 Protein Crystallization and X-ray Diffraction

Crystallization of biologically derived proteins is one of the most daunting tasks that depend on a number of factors i.e. purity and stability of protein, crystallization conditions, temperature or the methods employed to set up crystallization.

The theory of crystallization is based on a phase diagram that basically shows different phases under which protein crystals are likely or not to form quality-diffracting crystals and dependent on crystallization method employed. There are four main crystallization methods used for crystallization set up namely i) Micro batch ii) Vapour diffusion iii) Dialysis and iv) Free interface diffusion as shown in the phase diagram in Figure 2 but the most widely used technique is vapour diffusion method(*12, 13*).

A protein solution is prompted to stay in solution up to a certain extent and changes state by changing the conditions surrounding it such as the temperature, pH of buffers, presence of precipitants and additives that may result to formation of crystals(*12, 14*). When it is under-saturated, the protein remains in solution and possibility of crystal formation is raised if the protein is concentrated beyond the solubility limit. However, if the protein is supersaturated the probability of forming crystals is also reduced due too much precipitation. Crystal formation is possible in the nucleation/labile zone but may not be of good quality for X-ray diffraction due to fast nucleation rate. Where there is slower protein nucleation but still saturated, there is a probability of forming large quality diffracting crystals. This is referred as the metastable zone(*13, 14*) as illustrated on the phase diagram **below** dependent on crystallization method.

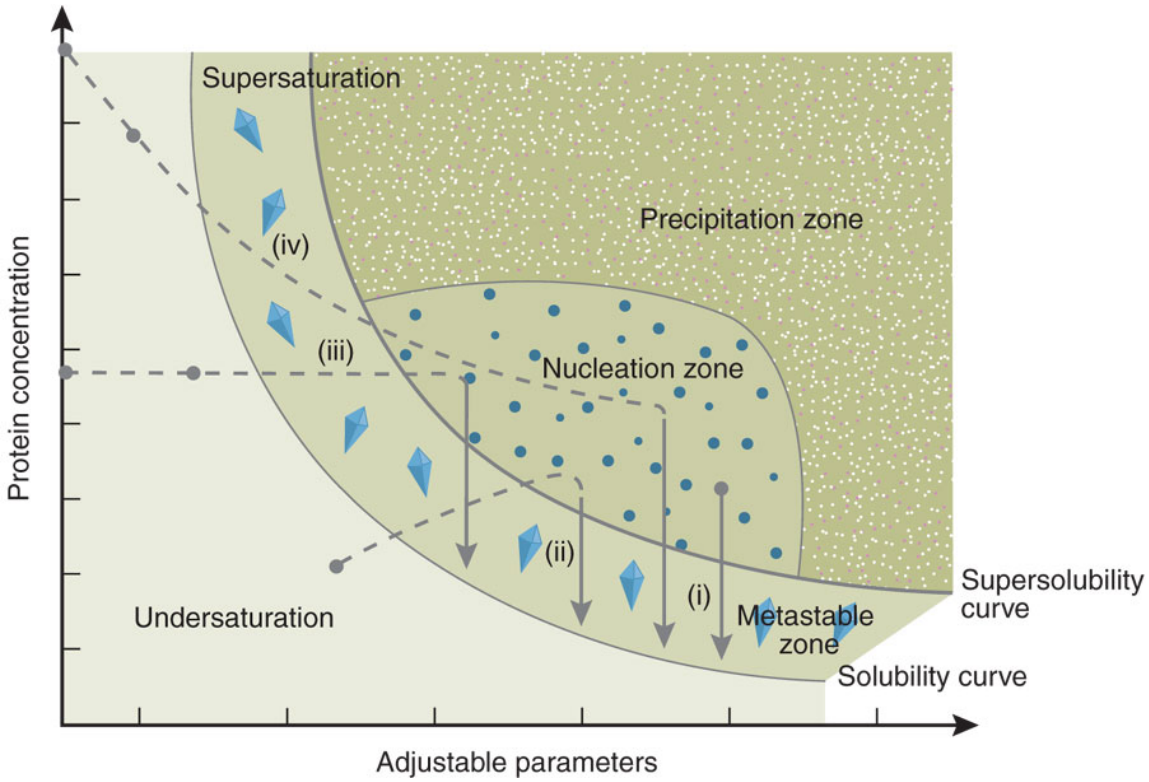

Figure 2: Schematic representation of a protein crystallization phase diagram showing different crystallization routes adapted by crystallization methods, i) micro batch ii) vapour diffusion, iii) dialysis, iv) free interface diffusion(*13*)

In this project, Vapour diffusion method was used i.e. both hanging drop and sitting drop vapour diffusion methods. Sitting drop vapour diffusion method is commonly used for crystallization screens with varied or random conditions in 96-well plates and may be automated using robotics for nanomolar measurements with reduced errors.

On the other hand, both sitting and hanging drop vapour diffusion are used for optimization of crystallization conditions varying pH, salts, precipitants, additives etc. referred as a grid screen.

When using a typical hanging drop vapour diffusion method, 0.5-I ml reservoir solutions with different pH, salts and precipitant concentrations are prepared in 24-well plates. A concentrated protein droplet is mixed with some volume of a reservoir solution on a coverslip and inverted into 500µl to 1ml mother liquor wells tightly sealed with high-vacuum grease. In a sitting drop method, the protein drop usually sits on a support above the reservoir solution but still tightly covered with high-vacuum grease using a coverslip or tape. The low concentration of the reservoir solution on the protein than in the well causes a diffusion gradient and water leaves the

protein drop to the reservoir causing a gradual increase in protein saturation and subsequently may yield to crystal formation(*12, 13*).

Once protein crystals are formed, the 3-dimensional structure of the protein can be determined using X-ray diffraction. Protein crystals have repetitive symmetric formation in the crystal lattice. Flash cooled protein crystals can be exposed to a continuous and accelerated spectrum of X-rays causing the electrons in the crystal lattice to oscillate causing interference with one another. The incident X-ray beam is diffracted at specific angles and the resultant constructive interference can be recorded on a detector as a pattern of dots depending on the quality of the protein crystal lattice(*12*).

2 Literature Review

2.1 Parasite Biology

The genome projects of *P.vivax* and *P.falciparum* as well as other plasmodium species have been completed and have given insights concerning similarities and differences that exist between the species. In particular, *P.falciparum* is highly A+T rich exhibited in over 80% of its genome whereas the *P.vivax* shows regions of A+T abundance and other regions that are G+C rich in content but with most gene families located in the A+T region. There is a lot of homology that exist between the two species especially the metabolic pathways but the *P.vivax* seems to possess quite unique and diverse pathways contributed by expanded gene profile for evading the host immune system than the *P.falciparum* during the parasite infection cycle(*6, 8*).

Plasmodium falciparum infectious cycle occurs in the blood stage during the life cycle of the parasite caused by thousands of mature merozoites that infect red blood cells (RBCs). Accumulation of infected RBCs also causes their agglutination to uninfected ones forming rosettes, which are susceptible for immune destruction. This is due to a series of immune responses causing production of pro-inflammatory mediators to combat accumulated parasite levels in RBCs such as TNF-α IL-12 and IFN- γ for parasite killing but also raises anti-inflammatory mediators associated with host cells damage that attack infected and uninfected RBCs causing massive hemolysis resulting to very low hemoglobin levels causing severe anemia and accumulation of hemozoin, an insoluble and toxic hemoglobin product formed from RBCs destruction by macrophages and has been associated with bone marrow suppression in young children(*3, 15, 16*).

Clinical symptoms of severe *P.falciparum* include chills, fever, metabolic acidosis and hypoglycemia. High parasite load is associated with high lactate production contributed by both host and parasite load and causes metabolic acidosis and increased glucose uptake that leads to hypoglycemia whereas fevers and chills are associated with an activated host immune response. High *P.falciparum* parasite load has also been shown to lead to infected RBCs accumulating in major organs such as the brain, liver, spleen and placenta that cause severe malaria cases like cerebral malaria whereas *P.vivax* frequent attacks causes endangered pregnancies due to severe anemia it predisposes pregnant women(*5, 16*).

Generally, *P.vivax* is not as severe as the *P.falciparum* and has not been extensively studied but is known to affect all populations and can have severe clinical implications caused by episodic attacks by the dormant hypnozoites in the liver. In addition, it is known only to infect reticulocytes, immature RBCs from Duffy positive reticulocytes that possess Duffy binding proteins for erythrocyte invasion and hardly infect Duffy negative blood group individuals; a population mostly localized in West Africa but can cause severe anemic cases due to massive destruction of reticulocytes (*5, 6*)

In a typical plasmodium life cycle (See Figure 3), a pregnant female anopheles mosquito takes a blood meal to support the developing gametocytes within her. In the process, it injects a stream of haploid sporozoites from its salivary glands into the host system, which travel to the liver cells via the blood stream and develop into schizonts and initially replicate asexually in the liver, a stage known as exo-erythrocytic schizogony then released into circulation where they infect RBCs and form ring-stage trophozoites which fully develop into schizonts inside RBCs; intra-erythrocytic schizogony, they rupture and release thousands of merozoites. In the *P.vivax*, the sporozoites either develop into dormant states known as hypnozoites, which remain in the liver for months or years and can cause episodic attacks(*5*)associated with clinical symptoms or form schizonts. These are later released into the blood stream and once mature rupture and release merozoites.

Some of the merozoites develop sexually to form male and female gametocytes. These fuse to form zygotes that develop into elongate and motile ookinetes within the mosquito gut which swim through the mid-gut and develop into oocytes, which develop and rupture to release thousands of mature sporozoites that penetrate the salivary glands of the mosquito ready for another injection into the host system during the next blood meal.(*17, 18*).

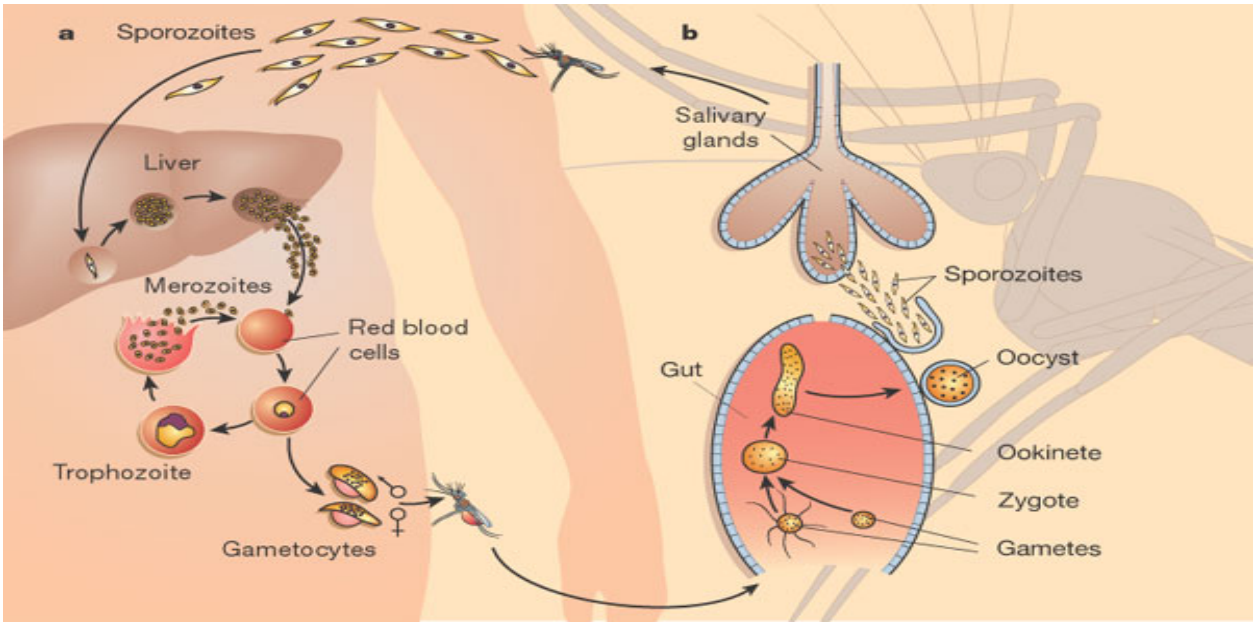

Figure 3: *Plasmodium falciparum* life cycle in human host and mosquito vector *Image source Nature Journal(17)*

2.2 Dihydroorotate Dehydrogenase

Dihydroorotate Dehydrogenase (DHODH) is an essential enzyme of the *De novo* pyrimidine pathway. It catalyzes the fourth rate limiting step and the only redox reaction in the pathway that converts l-Dihydroorotate to orotate mediated by different co-factors in diverse organisms (Figure 4**).**

The enzyme is present in both prokaryotes (gram-positive bacteria) and eukaryotes either as a cytosolic or membrane bound enzyme classified into two distinct classes, 1 and 2 respectively (*19, 20*). The class 1 DHODH enzyme predominantly uses Fumarate and NAD^+ as electron acceptors and localized in the cytosol. On the other hand, class 2 DHODH that also includes the gram-negative bacteria which is membrane-associated to the outer surface of mitochondrial membrane whereas the eukaryotic DHODH is localized in the inner mitochondrial membrane; uses FMN and Ubiquinone (Coenzyme Q) as electron acceptors and hence coupled to the mitochondrial respiratory chain(*21, 22*).

Class 2 DHODH is classified among the large superfamily of amidohydrolases believed to possess an α/β catalytic domain which is the core domain located at the C-terminus and characterized by alternating eight α helices and eight β sheets to make up an αβ fold in one

domain known as a "TIM" barrel fold possessed by most enzymes including the well known Triose Isomerase phosphate enzyme(*23-25*). In addition, this class of enzymes possesses an extensive N-terminal domain containing two α helices unlike their class 1 cytosolic counterparts. The N-terminus in eukaryotes is much longer than that found in gram-negative bacteria exemplified by *E.coli* DHODH and has been presumed to possess a signal peptide for proper mitochondrial localization and a trans-membrane helix for attachment to the outer surface of the inner mitochondrial membrane. Studies from eukaryote mutants DHODH lacking the signal peptide and trans-membrane helix N-terminus residues from both human and insect Drosophila melanogaster that share a sequence homology show improper localization and loss of in vivo activity but not in vitro (*20, 22, 26, 27*).

Plasmodium falciparum DHODH (*Pf*DHODH) is classified among the membrane bound, a class-2 Flavin-dependent enzymes that utilizes FMN in a redox reaction involving Coenzyme Q that is coupled to the mitochondrial respiratory chain. Genetic studies using a transgenic *P.falciparum* expressing Fumarate-dependent DHODH in yeast have shown that Coenzyme Q coupled to the mitochondrial bc_1 complex is very essential for the survival of *plasmodium falciparum* during the replicative blood stage as was observed from lack of slightest inhibition to the malaria drug, atovaquone whereas the wild type *P.falciparum* was inhibited within 48hours of running the inhibition assay thus indicating *Pf*DHODH as a valuable drug target(*28*).

The FMN is located at the α/β catalytic domain while the ubiquinone-binding site is located at the N-terminal domain. Studies show that the catalytic reaction involving the FMN and the ubiquinone occur via a non-sequential Ping-Pong mechanism whereby the FMN accepts electrons in one half of the reaction whereas a ubiquinone localized at N terminus accepts electrons in the second half reaction and regenerate FMN for subsequent reactions, depicting separate binding pockets for FMN and the ubiquinone(*29, 30*).

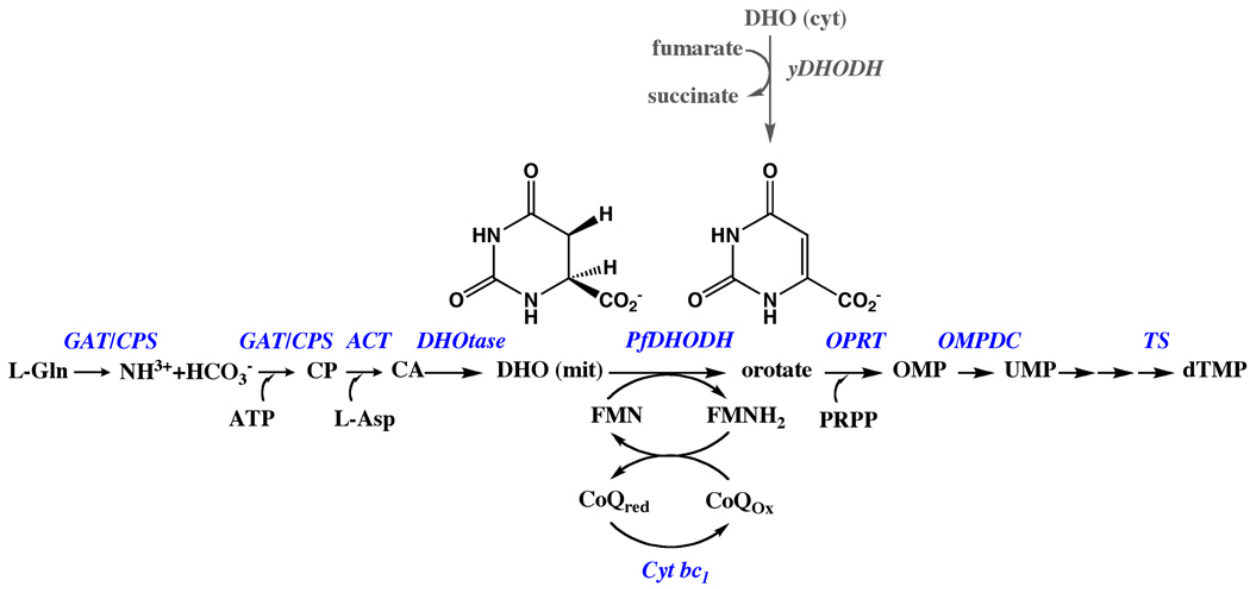

Figure 4:*Plasmodium falciparum* de novo pyrimidine biosynthetic pathway illustrating the *Pf*DHODH redox reaction involving FMN and Coenzyme Q cycle relying on cytochrome bc_1 complex from the mitochondrial respiratory chain; Yeast DHODH (yDHODH) relies on Fumarate as an electron carrier; Image source *Infectious Disorders - Drug Targets* (*31*).

*Pf*DHODH has been validated as a druggable target through homology to the human DHODH (*31, 32*) and its inhibition strategy and through studies against various inhibitors which are potential anti-malarial drugs including high throughput screening (HTS) of chemical scaffolds acting as potential inhibitors of the enzyme. It has also been shown to be selective against the human DHODH due to absence of a salvage pathway and variable N-Terminal α-helical domain where ubiquinone as well as inhibitors are believed to bind. Sequence and structural alignments show that the catalytic domain is conserved between the human and the parasite where the primary substrate binds but the ubiquinone binding site possesses different sequences with different inhibitor affinity and hence a strong candidate for parasite DHODH inhibition(*29, 31, 33, 34*).

2.3 *Plasmodium falciparum* and *Plasmodium vivax* Dihydroorotate Dehydrogenase

The 3-dimensional structure of the *P.falciparum* DHODH resolved by X-ray diffraction has a α/β fold at the catalytic domain with a longer N terminal domain comprising 2 α helices and 6 versions of the structure co-crystallized with different inhibitors are available in the Protein Data Bank, PDB IDs. 1TV5, 3165, 3168, 316R, 308A and 3SFK resolved between 2-2.4Å(*34-37*)

Crystallization of membrane proteins is one of the most challenging tasks due to the hydrophobicity of the residues spanning the membrane lipid bilayer. The class-2 membrane-bound DHODH enzymes are monotopic integral proteins i.e. attached on the outer surface of the inner mitochondrial membrane by part of their hydrophobic N-terminus α-helices. To enhance crystallization, recombinant *Pf*DHODH constructs have been produced with a deleted surface loop region (amino acids 385-415) and a truncated N terminal membrane-spanning domain located (158 amino acids) between the core domain and the presumed inhibitor-binding site. Studies have shown the truncation has no significant effect on the protein activity in vitro(*22, 27, 34*).

All resolved structures are N-terminally truncated and a surface loop deleted except one that only has the N-terminal membrane-spanning domain truncated. The surface loop is missing in DHODH from other species including the human DHODH, See sequence alignment in Figure 5 and has been shown to hinder crystal contacts when co-crystallized with inhibitors(*34, 35*). Comparison of *Pf*DHODH with the human DHODH structure reveals similar α/β catalytic domain but a variable N Terminal domain with variable inhibitor binding affinities due to different residues involved and thus species selective(*35, 38*).

However, purification of the N-terminally truncated *Pf*DHODH recombinant protein still require minimal presence of detergent in purification buffers due to the lipophilic environment of the secondary electron acceptor, Coenzyme Q and hence eliminates cases of protein aggregation and also maintains protein homogeneity(*39*).

On the other hand, there is no known resolved structure of *P.vivax* DHODH probably due to less studies done and lower severity of the malaria disease caused by this species as compared to *P.falciparum*. However there is an increasing need to step up studies including structure determination of *P.vivax* DHODH for structure-based drug design. This is due to increasing drug resistance to available anti-malarial drugs and also to find alternative efficacious drug for *P.vivax* malaria apart from the only standard Primaquine drug that has been shown to possess contra-indications to persons deficient in Glucose-6-phophate dehydrogenase and in pregnant women(*5, 40*).

P.vivax sequence superimposition with known A77 1726-Inhibitor bound *Pf*DHODH structure shows a close homology to *P.falciparum* DHODH inhibitor binding site and this is an initial lead showing same inhibitor binding strategy for anti-malarial drugs based on what is known between the human and *P.falciparum* DHODH structures (See Figure 7:Close-up view of *Hs*DHODH (A) and *Pf*DHODH (B) structures bound to A77 1726 inhibitor depicting different residues involved; and C shows a superimposed image of the *Pf*DHODH structure inhibitor binding site and *Pv*DHODH sequence.). However, structure determination is of outmost importance to clear speculations and to find more potent inhibitors for combating the malaria menace caused by *P.vivax* infections.

Most inhibitors that have been validated to inhibit the human DHODH are very poor inhibitors against the parasite DHODH(*35*) showing species-selectivity but there is also an ongoing research to find the most potent inhibitors for *Pf*DHODH by use of in silico drug design. Using the biological protein structure co-crystallized with synthesized chemical scaffolds as potential inhibitors (ligands), and use of computational studies is a new ground for lead optimization of anti-malarial drugs.(*34, 38, 41*)

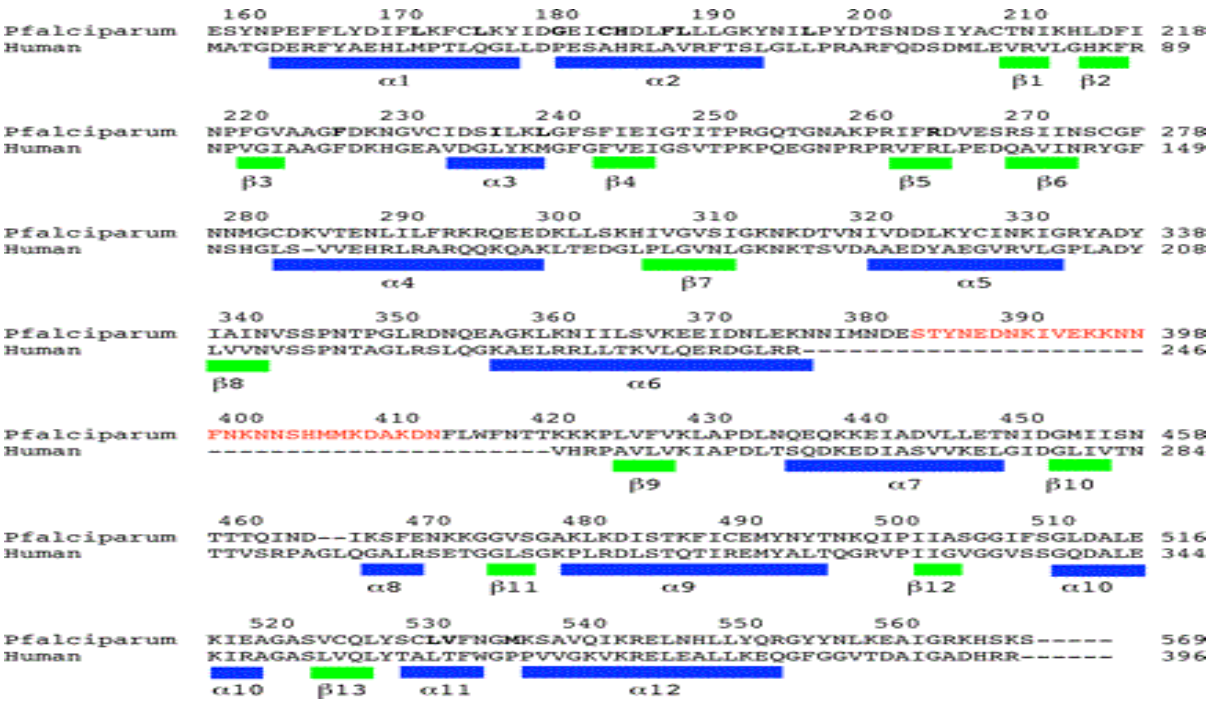

Figure 5: Sequence alignment of human and *P.falciparum* DHODH showing a surface loop (highlighted in red) but absent in the human DHODH (*34*)

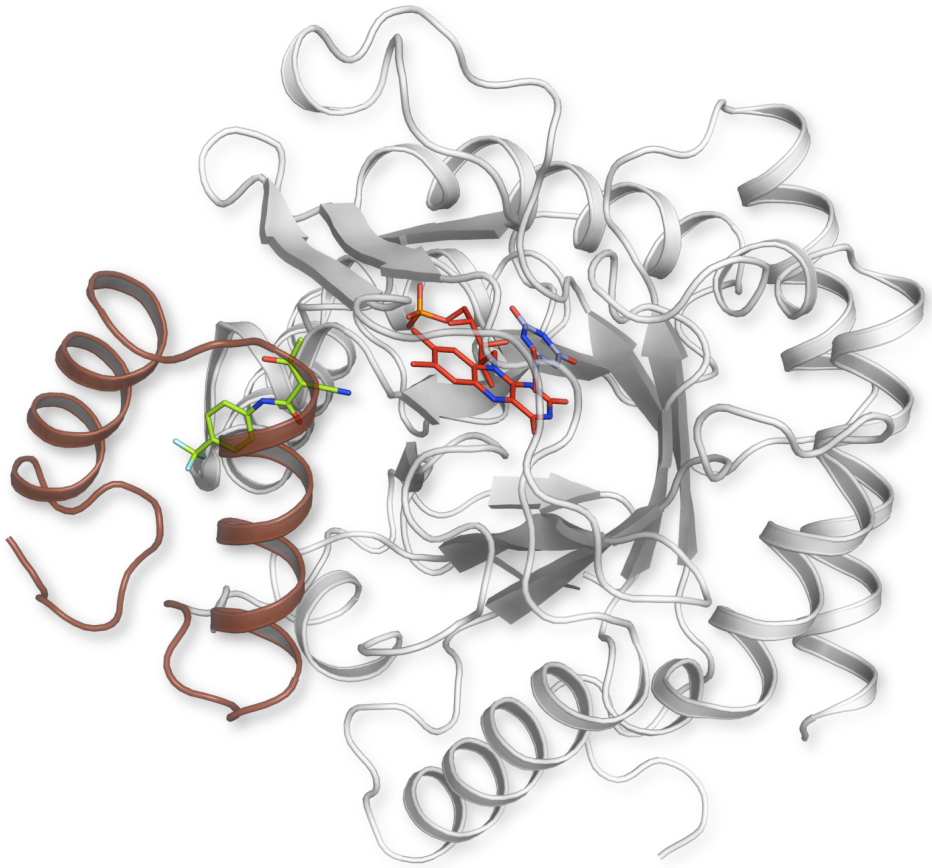

Figure 6: Overall *Pf*DHODH structure; C-terminal core domain (Grey) α/β motif with FMN (red) and orotate (blue) shown in sticks at close proximity; Small (Brown) α-helical N-terminal domain bound to an inhibitor (shown in green sticks). *Modified image; source(35)*

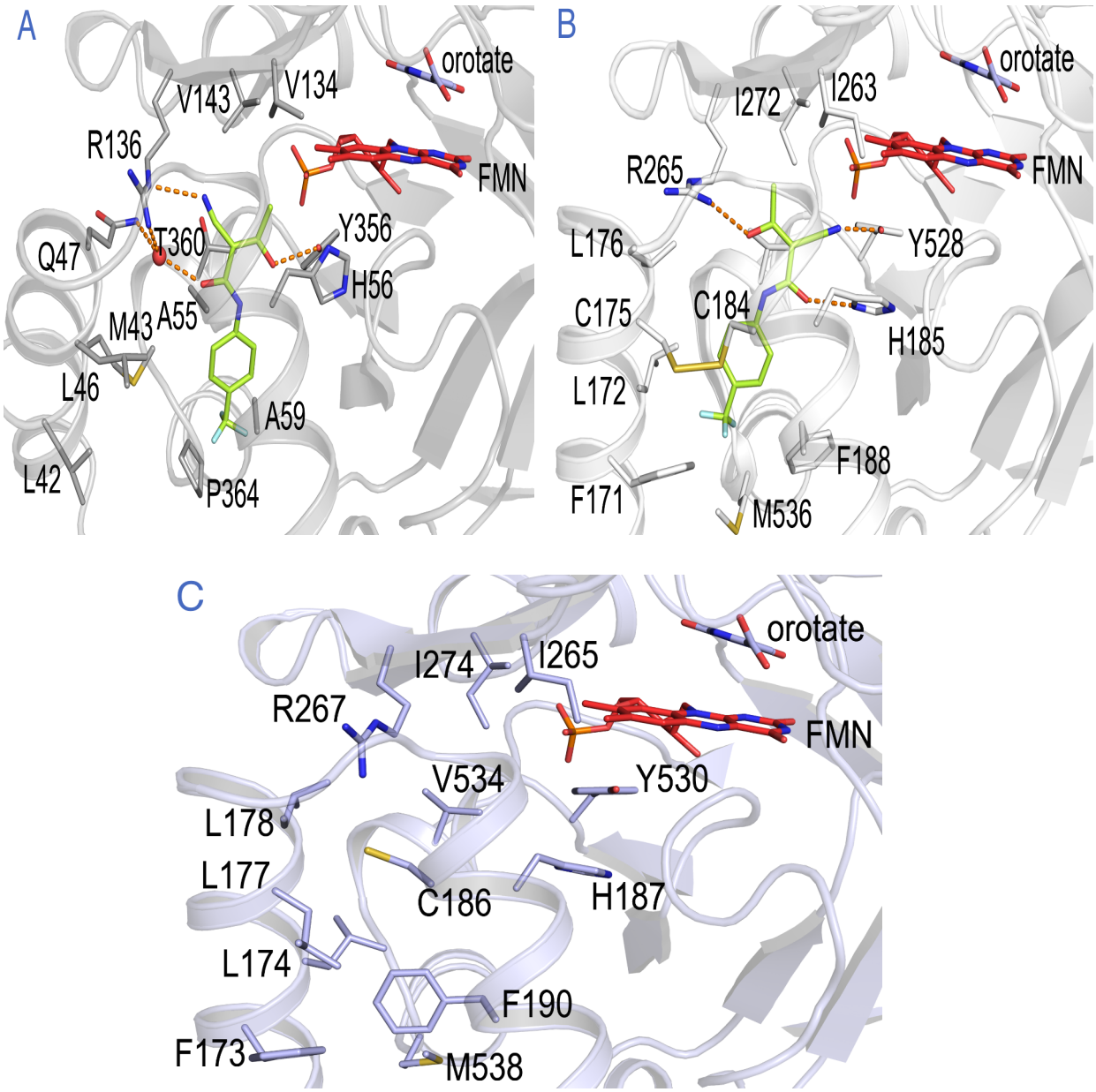

Figure 7:Close-up view of *Hs*DHODH (A) and *Pf*DHODH (B) structures bound to A77 1726 inhibitor depicting different residues involved; and C shows a superimposed image of the *Pf*DHODH structure inhibitor binding site and *Pv*DHODH sequence. Orotate, FMN and A77 1726 inhibitor are shown in blue, red and green sticks respectively. Side chain residues lining the quinone-binding site are shown in sticks. *Modified Images; sources(32, 35), PvDHODH montage by Swiss Model.*

3 Materials and Methods

All materials and reagents of the highest quality and purity were sourced from Sigma-Aldrich, Thermo-scientific, Qiagen or GE Healthcare unless otherwise stated.

All DNA concentrations were measured using Nanodrop ND-1000, Thermo-scientific; all western blots and all DNA-gels were analyzed using Fujifilm LAS-1000 Image Reader and DNA-UV trans-illuminator, Alpha Innotech, respectively.

3.1 Dihydroorotate Dehydrogenase Constructs

The genes for full-length *Pf*DHODH and *Pv*DHODH were initially synthesized and codon optimized for *E.coli* expression system (Geneart) as plasmids *Pf*DHODH-pMA and *Pv*DHODH-pMA respectively and different constructs cloned in the lab in pNIC28-Bsa4 vector.

Viable N-terminally truncated *Pf*DHODH (amino acids 159-569) and *Pv*DHODH (amino acids 161-573) constructs initially synthesized by project colleague were done by PCR-amplification using forward primers 5'-TACTTCAATCCATGTTGAAAGCTATAATCCGG-3' and 5'-TCCATGTTTGAAAGCTATGATCCGGAATTTTTTCCTG-3' respectively and a common reverse primer 5'-TATCCACCTTTACTGTTAGCTTTTGCTGTGTTTGC-3' and cloned in pNIC-28-BSA4 by ligation independent cloning. In addition, a surface loop was deleted from *Pf*DHODH (amino acids 385-415) *Pv*DHODH (amino acids 385-417) by Quick-change site directed mutagenesis using forward primers 5'-CAACATCATGAACGACGAGTTTCTGTGGTTCAACACCA-3' and 5'-GCAGCAATGGGTGGCGAA-3' and reverse primers 5'-TGGTGTTGAACCACAGAAACTCGTCGTTCATGATGTTG-3' and 5'-ATTTGCCCACGGTTCGCCACCCATTGCTGC-3' respectively. Resultant constructs have been abbreviated **pfa2b_6xhis** in Figure 19 and **Pvi-1** in Figure 22 (See *appendix A*) for use in this thesis.

3.1.1.1 N-Terminal Octa-histidine tagged Plasmodium falciparum Dihydroorotate dehydrogenase Construct

To make a longer his-tag, two histidines were inserted on the N-Terminal 6-histidine-tagged *Pf*DHODH construct by Quick-change Site-Directed mutagenesis kit (Stratagene). Initially primers were designed using quick-change software. A mutant strand was synthesized by PCR-amplification in a thermal cycler using forward primer 5'-ATATACATATGCACCATCATCATCATCATCATTCTTCTGGTGTAGATC-3' and reverse primer 3'-TATATGTATACGTGGTAGTAGTAGTAGTAGTAAGAAGACCACATCTAG-5' in a reaction with ~50ng double-stranded DNA template, dNTPs mix and pfuUltra high fidelity DNA Polymerase as summarized **below** and run for 18 cycles according to Stratagene protocol.

Table 1: Quick-change reaction Mix

Sample	Amount
10x Reaction buffer	5µl
dsDNA Template	~50ng
Forward primer	125ng
Reverse Primer	125ng
dNTPs	1µl
***PfuUltra* HF polymerase**	1µl(2.5U/µl)
ddH_2O	xµl=50µl

The reaction mix was then digested with 1µl *Dpn1* restriction Enzyme at 37°C for 1 hour to digest the methylated and hemi-methylated template (parental) DNA. Then 1µl of Dpn1 treated DNA was transformed in 50µl XL1-Blue supercompetent cells by heat-pulse method and 250µl of transformation reaction spread on LB-Agar plates supplemented with 50µg/ml kanamycin and incubated overnight at 37°C.

Colonies grew after >16hours and single colonies picked and grown overnight in 4ml LB media supplemented with 50µg/ml kanamycin and plasmid minipreps prepared using HP GenElute plasmid Miniprep Kit (Sigma-Aldrich) and sent to Eurofins MWG operons for sequencing to confirm which clones showed successful modification of the his tag in the construct, See **Figure 20.**

3.1.1.2 C-Terminal hexa-histidine tagged Plasmodium falciparum Dihydroorotate Dehydrogenase Construct

An attempt to make a construct with a 6-his tag on the C-Terminus of *Pf*DHODH was done by PCR-amplification and ligation independent cloning. Initially primers were designed using Serial cloner 2.1 software, to delete the N-terminal membrane-spanning domain from PfDHODH-pMA codon-optimized gene using the forward primer 5'-TTAAGAAGGAGATATACATATGTACTTCCAATCCATGGAGACCG-3' and to insert a 6-histidine tag on the C-terminus using the reverse primer 3'-AATTCTTCCTCTATATGTATACATGAAGGTTAGGTACCTCTGGC-5' by PCR amplification in presence of high fidelity phusion DNA polymerase, reaction buffer and dNTPs master mix and run in Eppendorf master cycler gradient as outlined in

Table 2**.** PCR-amplified samples were analyzed by running on 0.8% agarose gel at 100V for 30 minutes, stained in SYBR Stain and observed under the DNA UV-trans-illuminator.

To prepare the insert for ligation independent cloning, the PCR-amplified sample was PCR purified using the PCR Purification Kit (Qiagen) then ~1000ng or 500ng treated with T4 DNA Polymerase in presence of dCTP to create 12-15 base pair overhangs performed by the dual 3'-5'exonuclease-and 5'-3'polymerase activity of the enzyme.

Table 2: Thermal cycler Reaction conditions

Cycle step	Temp	Time	No. of cycles
Initial denaturation	98°C	30sec	1
Denaturation	98°C	10sec	25
Annealing	72°C	30sec	
Extension	72°C	30sec	
Final Extension	72°C	10min	
	4°C	Hold	

To prepare the vector, it was initially linearized by treatment with *Bsa1* Restriction enzyme while incubating at 37°C for 2 hours then running on 0.8% agarose gel and recovering the linearized vector by DNA extraction using QiAquick DNA Extraction kit. ~500ng or 250ng of plasmid was then T4 DNA polymerase treated in presence of dGTP to create overhangs complementary to those present on the insert.

Both T4 DNA polymerase treated insert and vector were PCR purified separately then mixed 50:50 and incubated at room temperature for 2 hours. An aliquot of the sample was then transformed in 50µl DH5α competent cells using heat-pulse method then spread on LB-Agar plates and grown overnight at 37°C. However, no colonies grew even after several attempts.

3.2 Protein Over expression

Protein over-expression was done using the successful, above-mentioned N-Terminally truncated and minus surface loop *Pf*DHODH and *Pv*DHODH constructs, **pfa2b_6xhis, pfa2b_8xhis and Pvi-1** respectively transformed in BL2I (DE3) *E.coli* strain. **(**See *appendix A* Figure 19**, Figure 21** and Figure 22).

3.2.1 Small-scale expression

Initial attempts to over-express the *Pf*DHODH protein using the **pfa2b_6xhis** construct showed very low expression levels in LB media. Therefore, a small-scale expression in both LB and Terrific Broth media was performed. Overnight starter cultures for both **pfa2b_6xhis** and **pfa2b_8xhis** were each diluted 1:1000 in 50ml LB and Terrific Broth supplemented with 50µg/ml kanamycin. *Pv*DHODH protein test expression using **Pvi-1 construct** was done in LB media using an overnight starter culture diluted in 50ml sterile LB media supplemented with 50µg/ml kanamycin done in replicates with and without riboflavin supplement. These were incubated at 37°C with aeration at 220rpm and grown to $O.D_{600}$ 0.6,sampled then induced with 1 mM IPTG and further grown at 20°C for 3 hours with sampling after every hour.

Samples were analyzed by running both uninduced and induced samples on SDS PAGE gels to observe the expression profile and determine best expression conditions for subsequent large-scale expression.

3.2.2 Large-scale expression

Each overnight starter culture grown from LB-agar transformants or glycerol-stocked freeze cultures was diluted 1:1000 in 800ml of either sterile LB or Terrific Broth media supplemented with 50 µg/ml kanamycin in 5L Erlenmeyer-flasks and grown at 37°C with aeration at 220rpm between $O.D_{600}$ 0.6-0.8; cultures were sampled then induced with 1 mM IPTG for protein expression and cells were grown overnight at 20°C with vigorous aeration at 220rpm.Further sampling was done before cell pellet harvest for expression analysis by running an SDS PAGE.

3.2.3 Cell pellet harvest

The overnight cell cultures were harvested by centrifugation at 4000xg for 30 minutes in Beckman Avanti J-26 XP centrifuge, JLA 8.100 rotor type. The cell pellet was recovered by discarding the supernatant and the resultant cell pellet from each construct was weighed and kept on ice before immediate cell lysis or kept at -80°C for long-term storage before the next step of cell lysis.

3.2.4 Cell lysis

Each cell pellet from *Pf*DHODH protein over-expression was resuspended in a lysis buffer (100mM HEPES pH 8.0, 500mM NaCl, 10% Glycerol, 0.05 %(w/v) THESIT detergent) according to modified Deng et al(*34*) protocol and a protease inhibitor added, homogenized and cells disrupted using a French press, all processes done on ice. To reduce the viscosity of the cell lysate caused by nucleic acids present, an aliquot of benzonase enzyme was added to the lysed cells during homogenization.

For the cell pellet derived from *Pv*DHODH protein over-expression, it was resuspended in a lysis buffer (IM NaCl, 100mM HEPES, pH 8.0,10mM DTT and 0.05%(w/v) THESIT detergent), non-EDTA protease inhibitor and benzonase added whereas cells sonicated according to Hurt et al modified protocol(*35*). Each cell lysate was clarified by centrifugation in an ultracentrifuge at 45000 rpm for 45 minutes and the supernatant collected in falcon tubes and kept on ice.

3.3 Protein Purification

3.3.1 Immobilized Metal Affinity Chromatography (IMAC) purification

Since the *Pf*DHODH and *Pv*DHODH constructs were cloned with histidine tags, the samples were purified by loading on an IMAC column connected to a FPLC ÄKTA system or by manual Ni^{2+} agarose resin in polypropylene columns.

Initial purification of a protein sample from **Pfa2b_6xhis** construct was loaded on a histrap column pre-charged with Ni^{2+} ions and equilibrated with Lysis buffer A (100mM HEPES pH 8.0, 150mM NaCl, 10% Glycerol, 0.05 %(w/v) THESIT with 5mM Imidazole) and the protein eluted with lysis buffer B (100mM HEPES pH 8.0, 150mM NaCl, 10% Glycerol, 0.05 %(w/v) THESIT with 400mM Imidazole) using a linear gradient between 20mM-400mM imidazole(*34*).

Subsequent cell lysis and purifications of protein from **Pfa2b_6xhs and Pfa2b_8xhis** construct were done in buffers with higher salt concentration i.e. 500mM NaCl since the preliminary purifications indicated poor binding to the Ni^{2+} column. In addition, all subsequent IMAC purifications were done manually due to better binding. This was done by incubating the protein with pre-washed 1ml Ni^{2+}-agarose resin for 1 hour at 4°C and eluting protein fractions with lysis buffer with different imidazole concentrations within a range of 5mM-200mM concentrations.

Purification of *Pv*DHODH protein expressed from **Pvi-1** construct was also done manually using Ni^{2+}-agarose resin as previously done but with a buffer (IM NaCl, 100mM HEPES, pH 8.0,10mM DTT and 0.05%(w/v) THESIT detergent modified from Hurt et al(*35*) with different imidazole concentrations within a range of 20mM-200mM concentrations.

After every step of IMAC purification, protein analysis by SDS PAGE was run to verify the fractions containing protein of interest. These fractions were pooled in a vivaspin sample concentrator (Sartorius Stedim) with 30kDa MWCO and concentrated to 500µl before loading on a superdex 200(10/30) gel filtration column or concentrated to 2.5ml when using Hi-load16/60 superdex 200-gel filtration column.

3.3.2 Gel filtration Chromatography

Each protein sample from *Pf*DHODH was loaded on a gel filtration column packed with either a normal or Hi-load superdex 200 resin equilibrated with a gel filtration buffer (10mM HEPES, pH

7.8, 100mM NaCl, 1mM N, N-dimethyldodecylamine N-Oxide, 5% Glycerol (v/v), 10mM DTT. Fractions corresponding to the protein peak were pooled in a vivaspin with 30kDa MWCO (Sartorius Stedim) and concentrated to 20mg/ml.

Protein samples from *Pv*DHODH were each concentrated to 500µl and loaded on superdex 200(10/30) column equilibrated with modified crystallization buffer(*35*), (15mM NaCl, 10mM HEPES, pH 7.4, 5mM Octyl- β-D-thioglucopyranoside; CMC=9) whilst fractions collected in 96-well blocks.

3.4 Protein Analysis

Protein analysis after purification is resolved by denaturing SDS PAGE. This method clearly indicates the purity of the sample as well as the molecular weight of the protein of interest can be verified. SDS PAGE can also indicate the expression profile on the target protein before and after induction with IPTG. To further verify if the purified fractions contain the protein of interest, a more sensitive method known as a Western blot is carried out.

3.4.1 SDS PAGE Analysis

3.4.1.1 Whole cell extracts prep

An aliquot of 1ml samples taken before and after induction with IPTG were spanned down at 12000rpm for 5 minutes in a micro-centrifuge and supernatant discarded. They were then fully resuspended in 120µl 1x SDS PAGE loading buffer (pre-heated 30 µl 4x LDS loading buffer, 60 µl 0.1 M DTT (16 mg/ml), 30 µl H_2O). Cells were then heated at 95°C for 5 minutes in a heating block and spanned down briefly before loading on an SDS PAGE pre-cast gel.

3.4.1.2 Protein fractions from IMAC and gel filtration purification

Samples from purification fractions were diluted with 4x LDS loading buffer and 10µl aliquots loaded on a SDS PAGE gel, as well as a standard protein ladder and run in 1x MES running buffer (20x MES=50mM MES, 50mM Tris Base, 0.1% SDS, 1mM EDTA, pH 7.3) at 200V for 35 minutes. The gel was then rinsed thrice with ultrapure water with heating in a microwave followed by brief incubation times on an orbital shaker each time. The gel was then stained with

SimplyBlue™ Safestain (Invitrogen) with further incubation for 10minutes then destained in ultra pure water for background clearance and better visualization of bands.

3.4.2 Western Blot Analysis

Protein samples from the expression and purification steps were run on SDS PAGE as described above then electro-blotted onto a nitrocellulose membrane for 1 hour at 100V.The membrane was then treated using one-hour western detection kit (Genscript). Each membrane was treated with equally mixed pre-treat solutions A and B for 5 minutes, rinsed in a 1x wash solution and incubated with a prepared primary anti-his monoclonal antibody solution on an orbital shaker for 40 minutes at room temperature. This was then rinsed and washed with 1x wash solution thrice with 10 minutes incubation times on an orbital shaker after each washing. Each membrane was then treated with a prepared chemiluminescent HRP substrate working solution and incubated for 3 minutes then visualized under the Fujifilm LAS-1000 chemiluminescent Image Reader for his-tagged protein signal detection.

3.5 Crystallization set-up and Crystal screening

Vapour diffusion method was used to set up random crystallization screens and grid screens for purified and concentrated protein of *Pf*DHODH to 20mg/ml derived from both constructs but none for *Pv*DHODH. Initially a sparse matrix crystallization screen was set up using structure screen kits (Molecular Dimensions; MD1-01 and MDI-02) in SwissSci 96-well plates in sitting drop format using a robot. These were sealed with vacuum tape and kept at 20°C and examined under the microscope after 24hours for any crystal growth in the wells. Grid screens were set up using hanging drop vapour diffusion method in 24-well plates based on previous known conditions used for *Pf*DHODH protein and from the sparse matrix hits.

A hit was identified with conditions; 0.1M Na HEPES buffer, pH 7.5 and precipitant 0.8M Na dihydrogen phosphate/ 0.8M K dihydrogen phosphate from a plate set up using protein expressed and purified from **Pfa2b_8xhis** construct and was used to optimize crystallization conditions by varying the pH of the buffer between 6-7.5 and precipitant ranging between 0.4M-1.4M in 1ml reservoir solutions in 24-well plates. In addition, other grid screens were set up based on Deng et al(*34*) modified ammonium sulphate crystallization conditions and Leeds group unpublished crystallization conditions. A concentrated protein sample from each construct was pre-mixed

with orotate [natural substrate in DMSO (50mM)] to a final concentration of 1mM and an inhibitor [DC413 solubilized in DMSO (25mM)] to a final concentration of 0.6mM and then 1µl or 1.5 µl protein drop was pipetted on a glass cover slip and mixed with an equal volume of the 1ml reservoir solution from respective wells and inverted as hanging drops, sealed with high vacuum greased and kept to saturate and grow at 20°C.

Crystals that grew in different grid screens conditions were picked with different loop sizes whilst cryo-protected, flash-cooled and stored in liquid nitrogen awaiting X-ray diffraction analysis.

Screening of crystals was done at the European Synchrotron Radiation Facility (ESRF) micro-focus beam line ID23-2 in Grenoble, France.

4 Results and Discussion

Constructs modification

To make a construct with a longer N-Terminal 8-histidine tag by Quick-change Site Directed Mutagenesis was successful as confirmed from the sequencing results in **Figure 20** (See *appendix A*). On the hand, an attempt to make a construct with a 6- his tag on the C-Terminus by ligation independent cloning did not work since no colonies grew. However, preparations of the insert and vector before T4 DNA polymerase treatment seem to work as observed on DNA agarose analyses **(**Figure 8).

Protein Expression

The protein expression profile of *Pf*DHODH constructs on both LB and terrific broth media indicated a better expression level in terrific broth than LB media as compared to initial attempts to express in LB media with indications of very low expression levels. Resultant large-scale protein over-expression in more enriched terrific broth gave larger cell pellet recovery with high protein amounts for subsequent protein purification (**Figure 9**). However, the protein expression levels differed between the two constructs **Pfa2b_6xhis** and **Pfa2b_8xhis** with the former yielding more protein content than the latter as observed in subsequent steps during protein purification. On the other hand, initial test expression of *Pv*DHODH in LB media indicated a good expression profile enough for scaling up to large-scale expression. However, cell disruption by sonication after large-scale over-expression was not effective in releasing the protein content as observed from the cleared lysate shown in **Figure 9, C** and **D.**

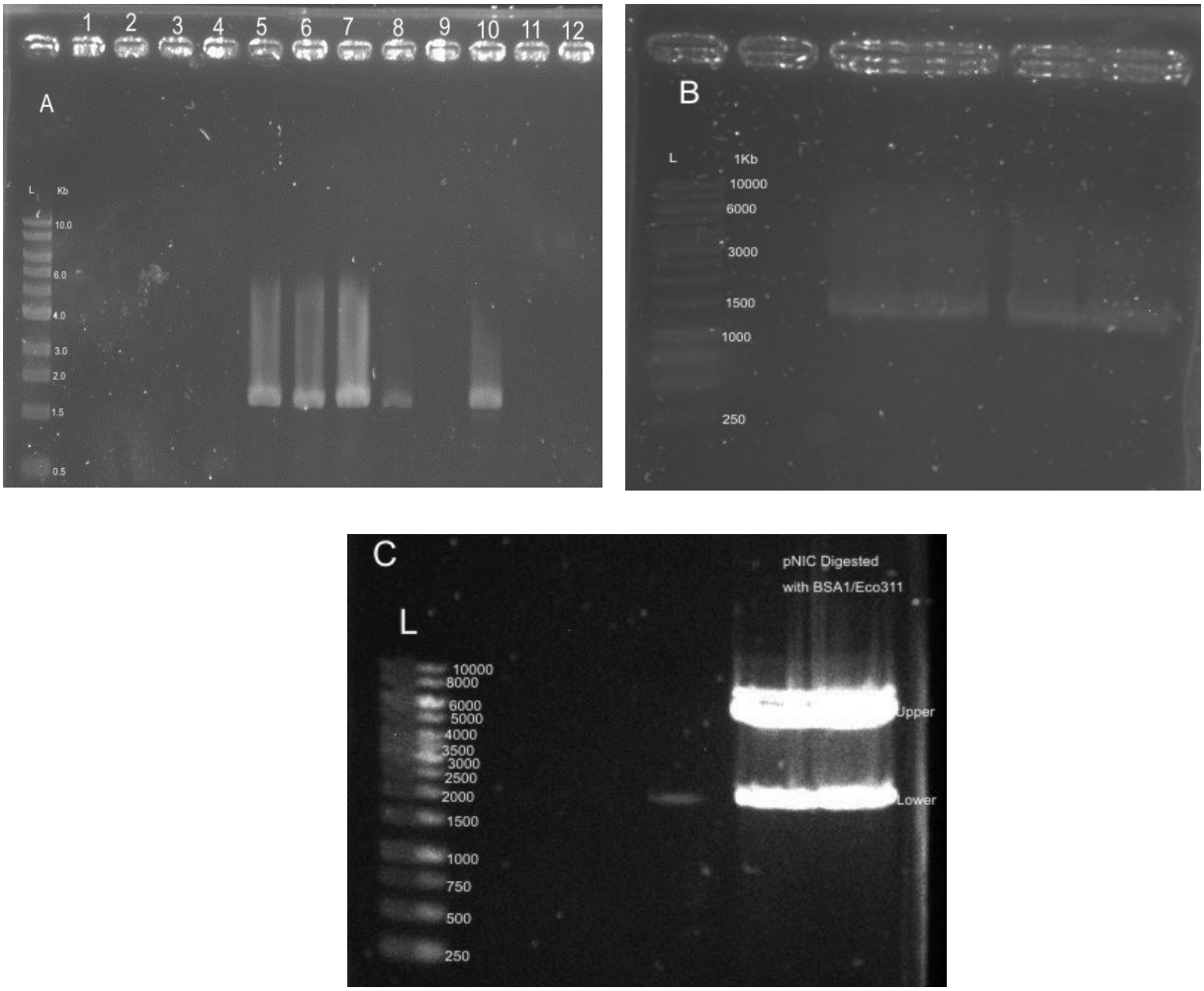

Figure 8: DNA gel analyses for both insert and Vector; A shows small scale PCR amplifications of insert in different PCR temperature gradients 1-12; B indicates large scale amplification of insert of ~1500bp using gradient 7 from small scale PCR amplification; C shows pNIC-28-bsa4 linearized with Bsa1 restriction Enzyme, upper band ~5000bp.

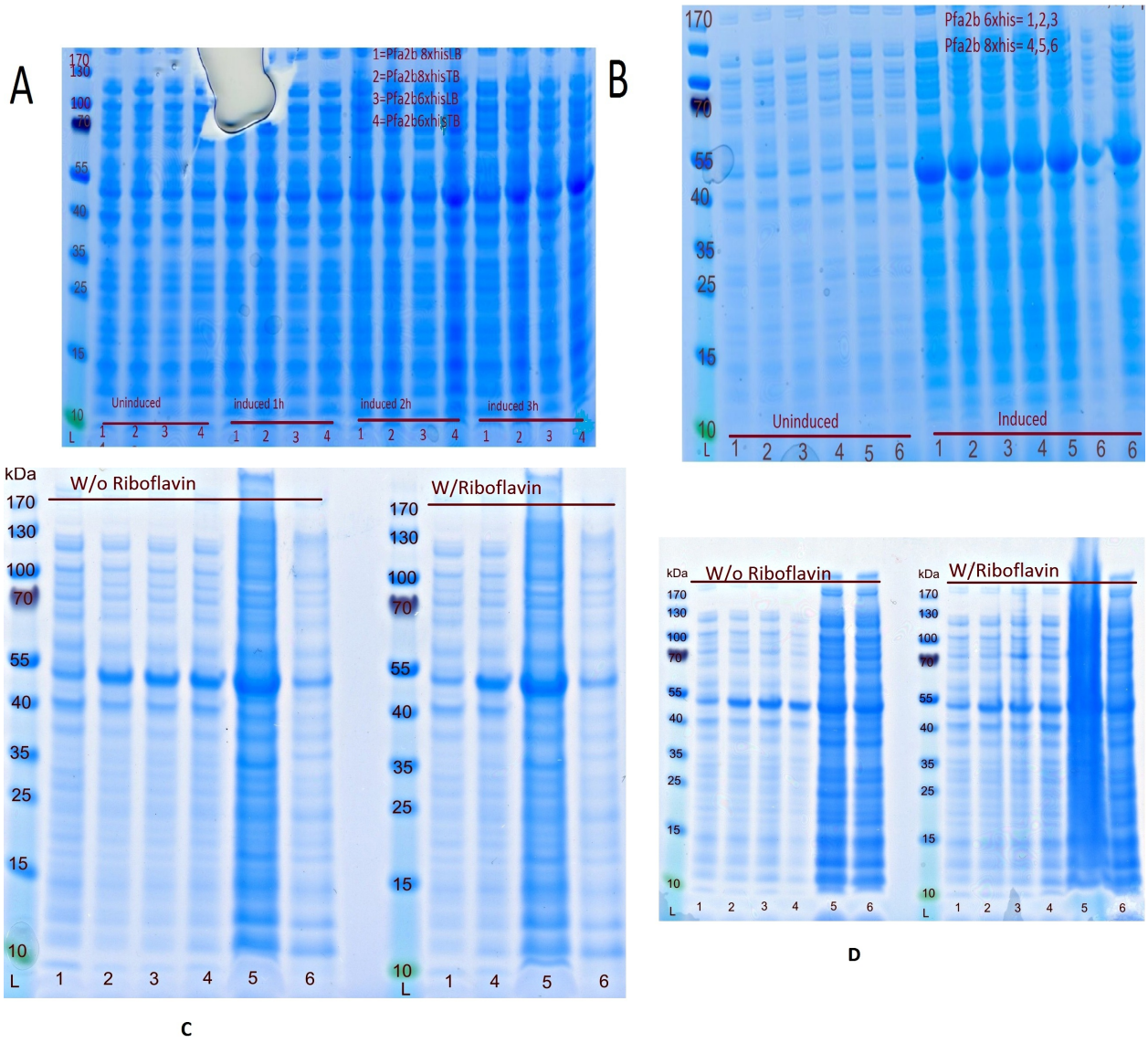

Figure 9: Small and large scale expression of *Pf*DHODH and *Pv*DHODH; A) shows small scale expression of *Pf*DHODH between 6-his and 8-his tagged constructs in LB and TB=terrific broth whereas B) indicates their overnight expression levels in terrific broth; C and D shows *Pv*DHODH small and large scale expression respectively supplemented with or without riboflavin. Lane 1=uninduced; induction lanes 2=after 1h, 3=after 2h, 4= after 3h, 5=whole lysate, 6=cleared lysate

Protein purification

Preliminary IMAC purification of *Pf*DHODH protein from 6g of cell pellet using both constructs indicated different imidazole elution profiles as observed from the SDS PAGE and western blot analyses shown in Figure 10 and Figure 11. Protein elution from the 6-his tagged construct is detectable on the western blot at about 20-30mM imidazole concentrations whereas on 8-his tagged construct, better elution is much more evident at about 60mM imidazole concentrations.

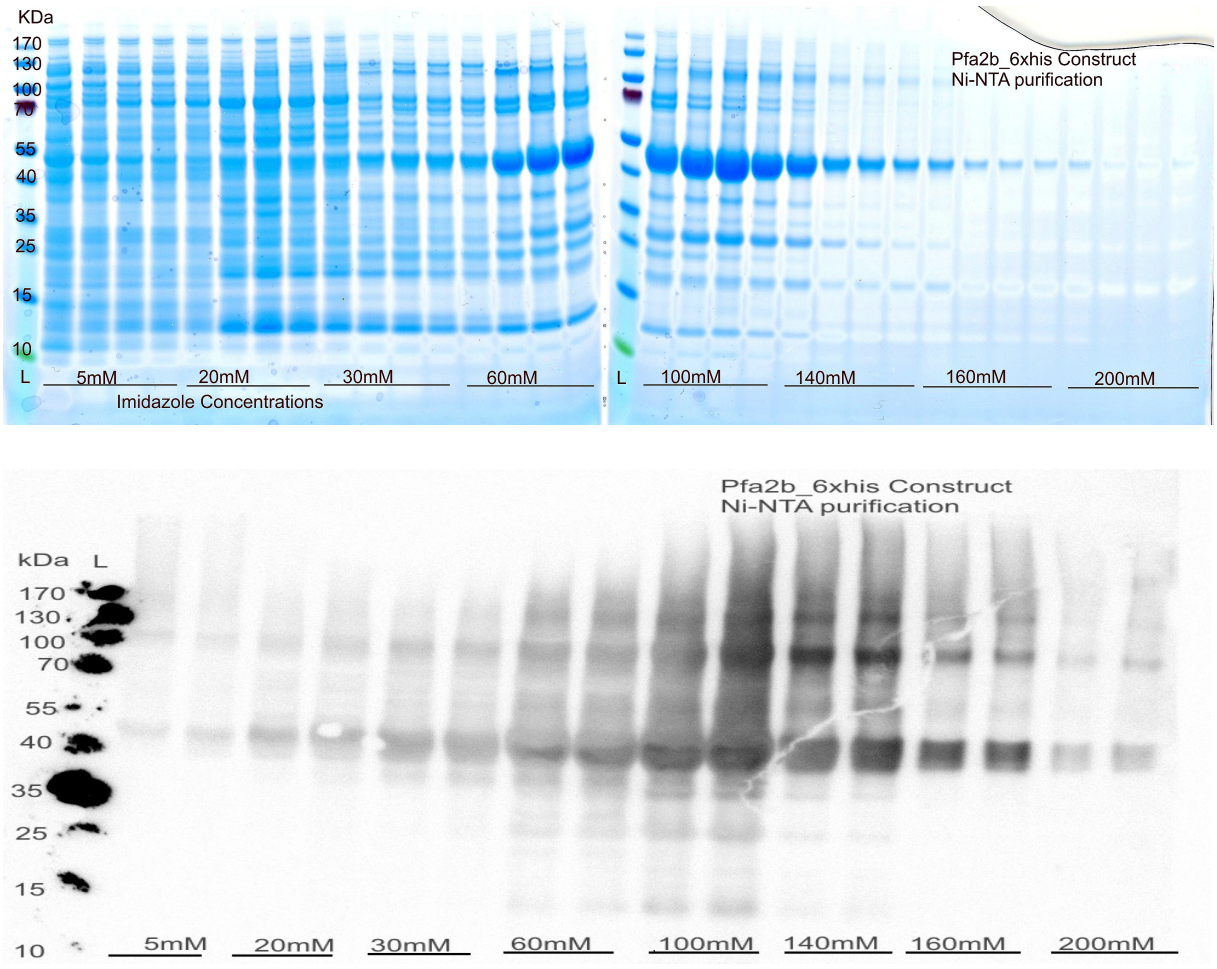

Figure 10: SDS PAGE and Western blot analyses showing IMAC purification of *Pf*DHODH protein from 6g of cell pellet cultivated using N-terminally truncated and minus surface loop Pfa2b_6xhis construct

However, despite the fact that the 8-his tagged construct indicated better interaction and binding to the Ni-NTA- agarose resin as observed on the western blots to separate the protein of interest from other proteins that might be present in the cleared lysate, the 6-his tagged construct indicated better protein expression in comparison to the 8-his tagged construct. This can be

observed from the SDS PAGE analysis **above** that shows quite high protein elution bands from 60mM imidazole concentrations in comparison to the 8-his tagged construct elution bands **below** derived from an equivalent 6g cell pellet.

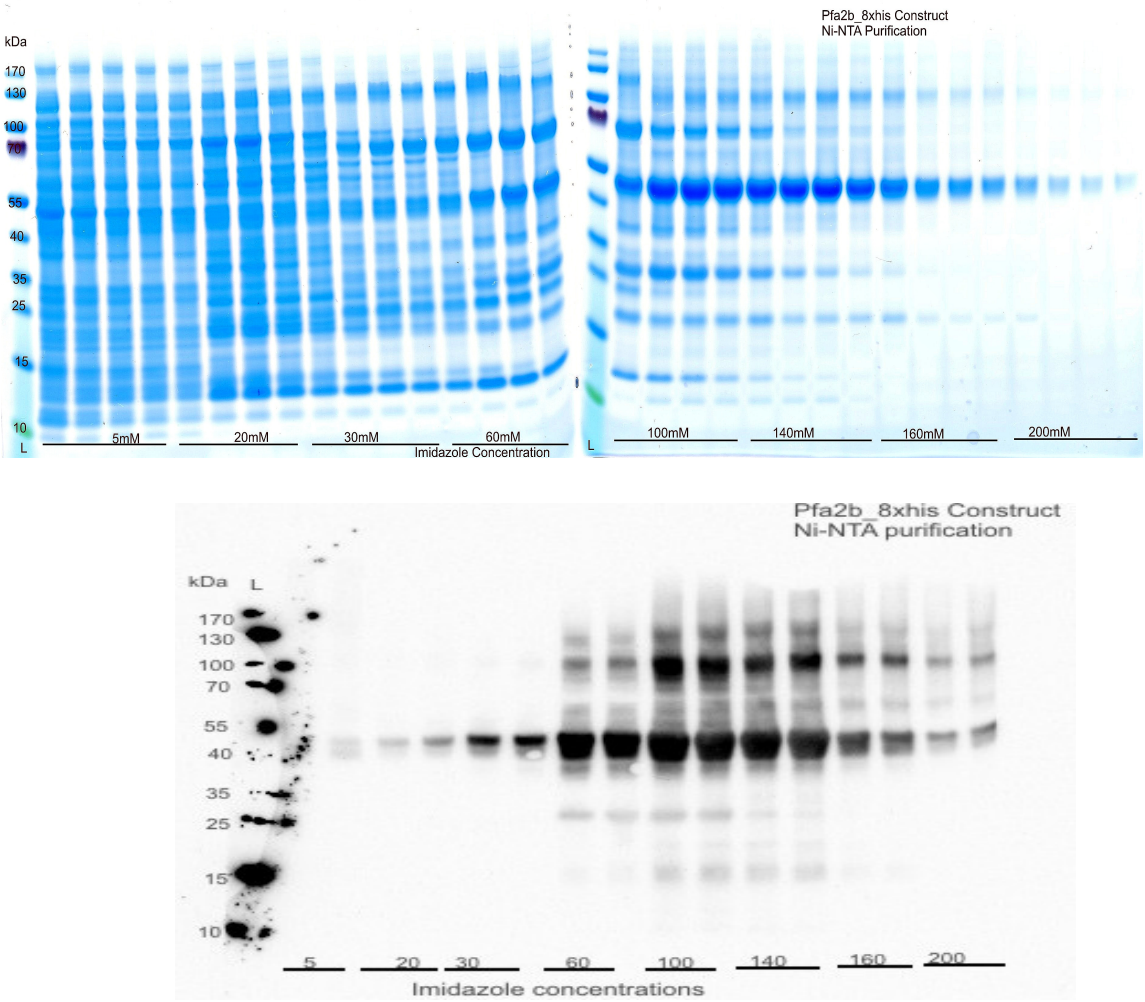

Figure 11: SDS PAGE and Western blot analyses showing IMAC purification of *Pf*DHODH protein from 6g of cell pellet cultivated using N-terminally truncated and minus surface loop Pfa2b_8xhis construct

IMAC purification from the *Pv*DHODH protein expressed in a 6-his tagged construct indicated protein elution from 60mM Imidazole concentrations as observed in Figure 12 though no western blot analysis was carried out to verify the efficiency of the his tag to bind to the Ni-NTA resin.

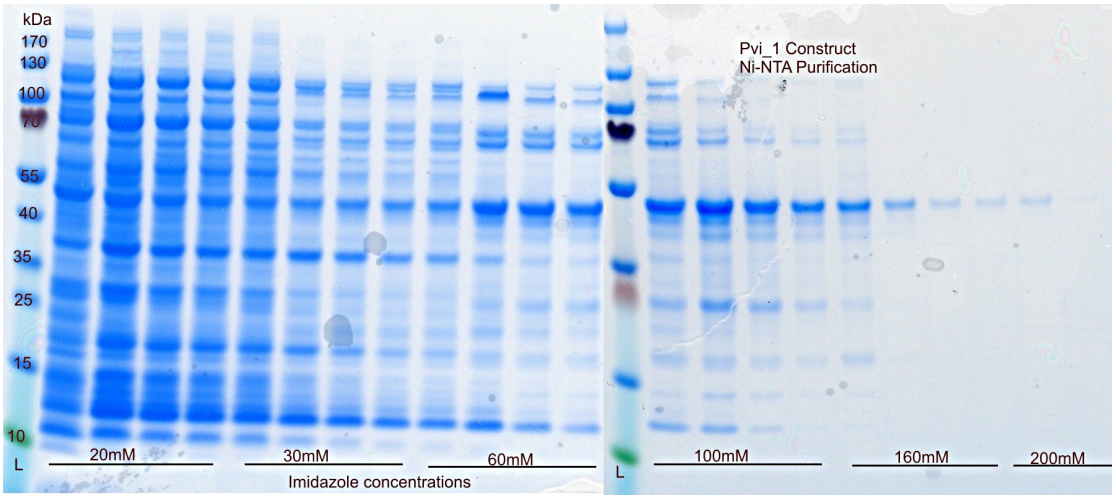

Figure 12: IMAC purification of *Pv*DHODH protein expressed from N-terminally truncated and minus surface loop Pvi-1_6xhis construct

Further purification of *Pv*DHODH protein corresponding to 60-160mM by gel filtration chromatography indicated inhomogeneous protein elution observed from the elution profile in Figure 13 but with presence of protein of interest of ~45kDa eluted from the initial peaks as a trimer analyzed by SDS PAGE. However, no western blot analysis was performed to verify the extra bands.

On the other hand, further purification of *Pf*DHODH protein expressed in 6-his tagged construct using superdex 200-gel filtration chromatography produced a good elution profile. However, subsequent analysis of fractions by SDS PAGE indicated presence of protein of interest of ~43kDa corresponding to the peak but with some indications of several uncharacterized bands as shown in Figure 14 and concentrating the protein peak fractions for crystallization set up did not yield any crystals. Further protein purifications expressed in both 6-his and 8-his tagged constructs did not indicate such a homogenous peak but yielded much pure samples by hiload gel filtration chromatography as observed on SDS PAGE and western blot analyses (Figure 15).

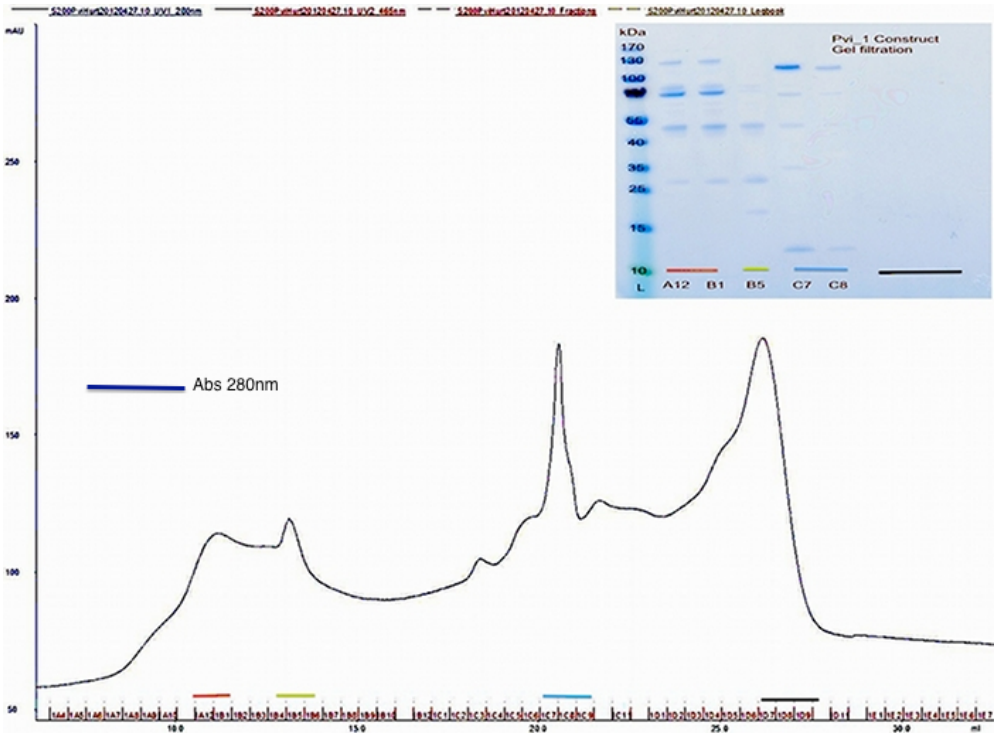

Figure 13: S200 Gel filtration chromatography and SDS PAGE analysis of *Pv*DHODH protein; initial peaks show a protein band of ~45kDa

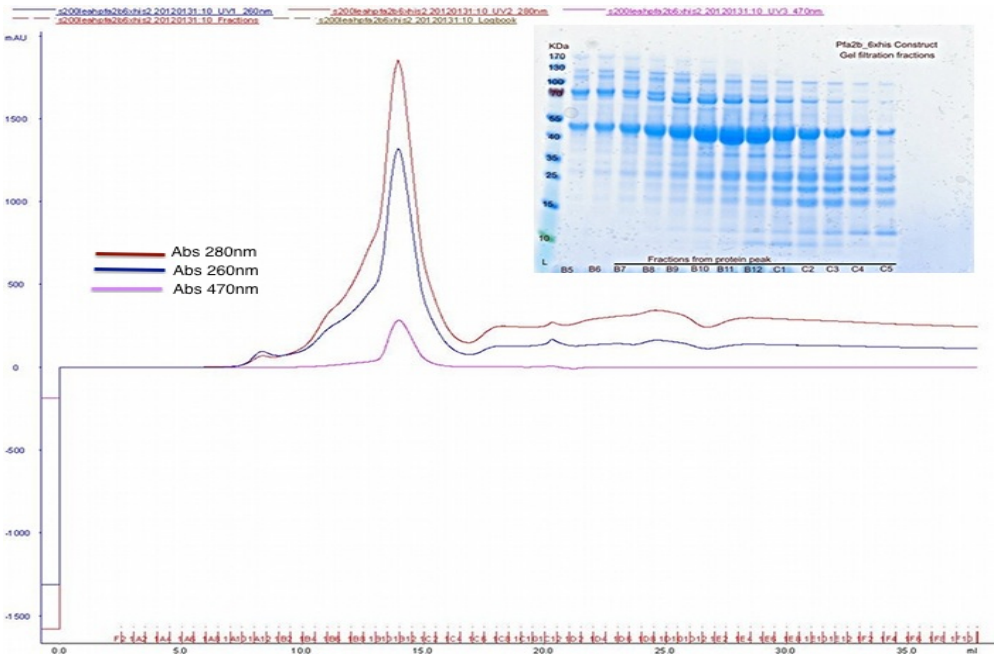

Figure 14: Preliminary S200 gel filtration chromatography of *Pf*DHODH protein expressed in 6-his tagged construct exhibited a good elution profile.

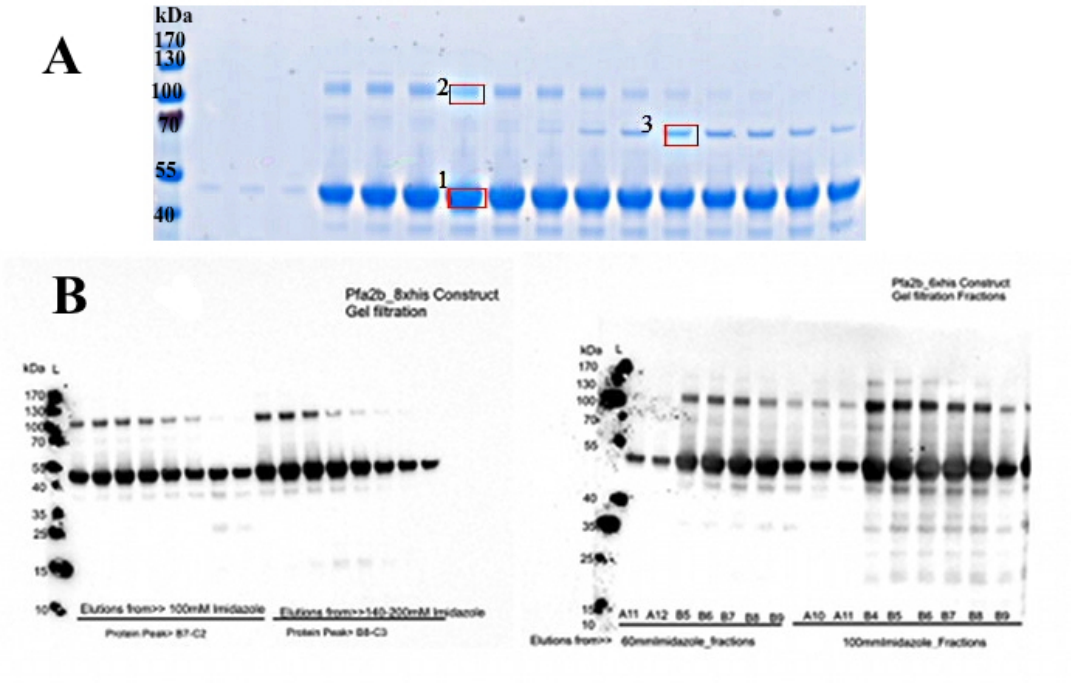

Figure 15: SDS PAGE and Western blot analyses of *Pf*DHODH protein from gel filtration fractions: A) shows SDS PAGE analyzed *Pf*DHODH protein fractions after hiload S200gel filtration step whereas B) western blotted protein samples indicating chemiluminescent signals detected at ~45kDa and ~100kDa.

SDS PAGE analysis of the inhomogeneous *Pf*DHODH protein peak expressed in both constructs indicated 3 distinct bands of ~45kDa, ~70kDa and ~100kDa but analysis by western blot only detected bands at ~45kDa and ~100kDa postulating the expressed protein likely being a dimer.

Further analysis of the SDS PAGE distinct bands by mass spectrometry and blasting the peptides sequences with both *E.coli* and *Plasmodium falciparum* libraries confirmed western blot findings. Peptide sequences corresponding to ~45kDa band gave *P.falciparum* hits but none for *E.coli* confirming *P.falciparum* expressed DHODH protein whereas the ~70kDa and ~100kDa bands gave both *P.falciparum* and *E.coli* hits (See *appendix B* supplementary data on Table 3).

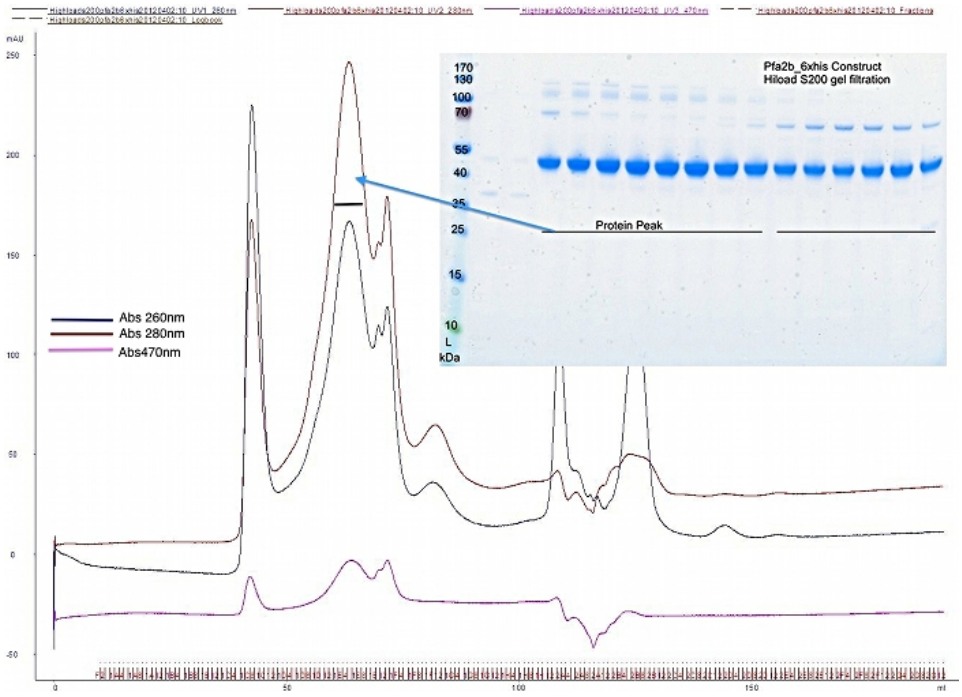

Figure 16: Hiload S200 Gel filtration chromatography elution profile and SDS PAGE analysis of *Pf*DHODH protein expressed in a 6-his tagged construct.

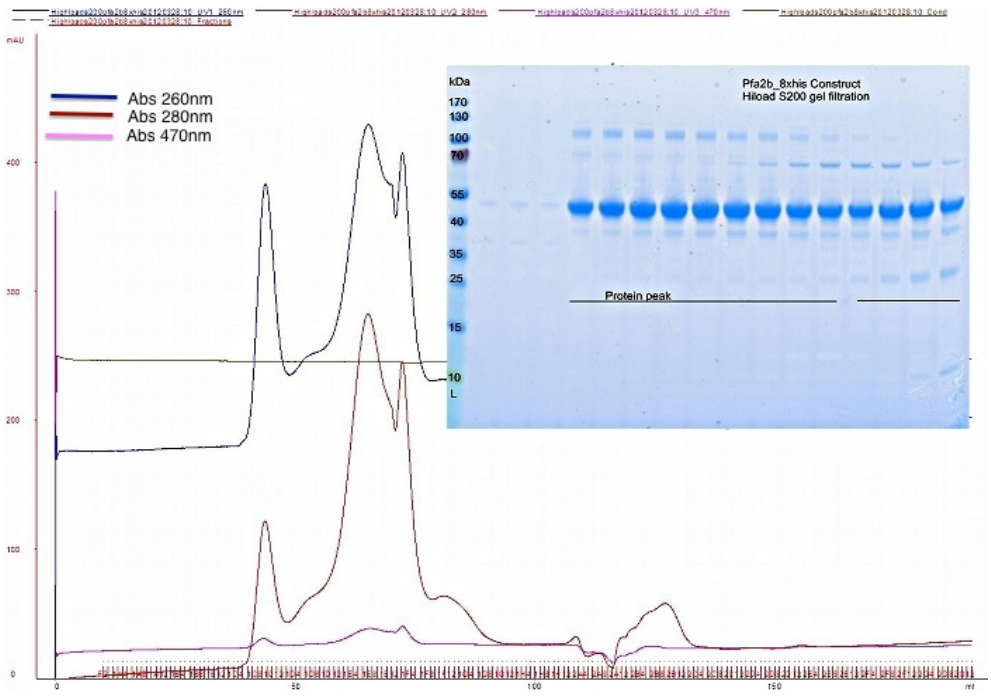

Figure 17: Hiload S200 Gel filtration chromatography elution profile and SDS PAGE analysis of *Pf*DHODH protein over-expressed in 8-his tagged construct.

In addition, the gel purified protein expressed using the 8-his tagged construct gave a cleaner sample than that expressed in the 6-his tagged construct but the latter yielded more protein than the former as observed on protein elution peak heights each derived from 12g of cell pellet (Figure 16 and Figure 17) confirming observations made during IMAC purification step.

Crystallization and X-Ray diffraction

Na/K Dihydrogen phosphate optimized sparse matrix hit using concentrated protein from twin peak in Figure 17 yielded crystals whereas *Pf*DHODH protein concentrated excluding the fractions containing the *E.coli* contaminants prominent bands from SDS PAGE analysis (Figure 16) using ammonium sulphate grid screen also yielded yellow needle-like crystals both shown in Figure 18**, A** and **B** respectively.

Analysis of the liquid nitrogen flash cooled crystals at the ESRF beam line ID23-2 in Grenoble, France, indicated the Na/K dihydrogen phosphate grown crystal were actually salt whereas the ammonium sulphate derived needle-like crystals indicated a viable diffraction pattern of ~6.8 Angstrom.

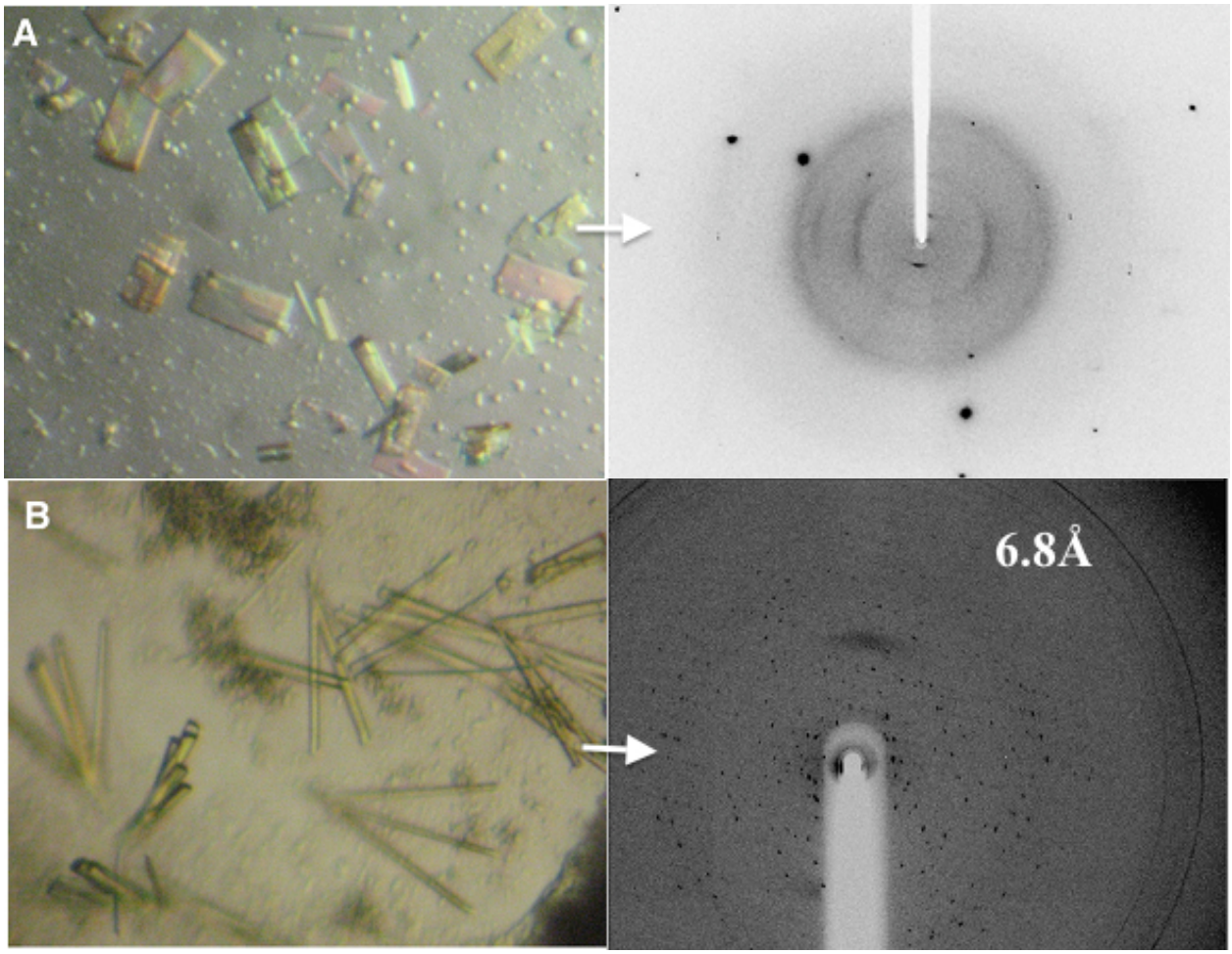

Figure 18: *Pf*DHODH crystals grown under different conditions with corresponding diffraction observed; A) shows salt crystals yielded from Na/K dihydrogen phosphate precipitant grid screen with no diffraction pattern; B) shows yellow needle-like protein crystals yielded from Ammonium sulphate precipitant grid screen that diffracted at ~6.8Å

5 Conclusions

Preliminary expression of *Pv*DHODH protein in LB media gave a good expression profile for large-scale over-expression in *E.coli* expression system. However, subsequent steps need to be optimized to give a pure and homogenous sample for setting up crystals.

For the *Pf*DHODH constructs, modification of the 6-his tagged construct to make a longer 8-histidine tagged construct by site directed mutagenesis was successful whereas the attempt to make a C-terminus 6-histidine construct by ligation independent cloning failed. LIC failure is most likely due to loss of material (vector and insert) after T4 DNA polymerase treatments

during PCR clean up resulting to very low plasmid concentrations for subsequent reaction and hence no viable colonies recovered after transformation.

Nevertheless, there was successful *Pf*DHODH protein over-expression in terrific broth media using both N-Terminus his-tagged constructs with the 6-his tagged construct yielding more protein than the 8-his tagged construct as observed in SDS PAGE analysis and gel filtration protein elution peak profiles. However, the latter indicated better binding on NI^{2+} resin during IMAC purification step.

Based on mass spectrometry scoring, *Pf*DHODH expressed protein might be likely a dimer initially purified by IMAC and co-purified with some *E.coli* proteins as shown in the supplementary data (*Appendix B*) subsequently detectable during gel filtration step. In addition, despite the likely slight aggregation observable by formation of void peaks during the gel filtration step, concentrating only the major protein fractions analyzed by SDS PAGE yielded relatively pure 20mg/ml protein that eventually formed viable diffracting crystals.

6 Future Perspective

For the *Pv*DHODH, protein purification protocol needs to be optimized by performing buffer and detergent screens since there are no known conditions in literature since attempts to use both human and *P.falciparum* DHODH known conditions failed to give a clean protein sample.

On the other hand, future target to obtain much better quality diffracting crystals for *Pf*DHODH for 3-dimensional structure elucidation, it is imperative to perform in vitro enzymatic assay to ensure there is no compromised enzyme stability and optimize purification steps to eliminate co-purified *E.coli* proteins and as well other contaminants. This can be done by an additional ion exchange purification step after gel filtration chromatography step or performing another IMAC purification after tag cleavage by the TEV cleavage site or use of cobalt resin for purification (*10, 42*). In addition, further optimization of crystallization conditions may also be necessary. Additives screen and micro- seeding may be a good option(*13*).

It is also important to further attempt making C-terminus his-tagged constructs for both *Pv*DHODH and *Pf*DHODH by LIC or conventional cloning for comparison purposes with the N-terminus his-tagged constructs in terms of protein expression levels and state.

7 References

1. WHO. (2010) World Malaria Report 2010, Geneva.
2. WHO. (2011) World Malaria Report 2011, Geneva.
3. Douglas J. Perkins, T. W., Gregory C. Davenport, Prakasha Kempaiah, James B. Hittner, and John Michael Ong'echa. (2011) Severe Malarial Anemia: Innate Immunity and Pathogenesis, *International Journal of Biological Sciences. 7*, 1427-1442.
4. Sabbatani, S., Fiorino, S., and Manfredi, R. (2010) The emerging of the fifth malaria parasite (Plasmodium knowlesi): a public health concern?, *Brazilian Journal of Infectious Diseases 14*, 299-309.
5. Mendis, K., Sina, B., Marchesini, P., and Carter, R. (2001) The neglected burden of Plasmodium vivax malaria, *The American Journal of Tropical Medicine and Hygiene 64*, 97-106.
6. Carlton, J. M., Adams, J. H., Silva, J. C., Bidwell, S. L., Lorenzi, H., Caler, E., Crabtree, J., Angiuoli, S. V., Merino, E. F., Amedeo, P., Cheng, Q., Coulson, R. M. R., Crabb, B. S., del Portillo, H. A., Essien, K., Feldblyum, T. V., Fernandez-Becerra, C., Gilson, P. R., Gueye, A. H., Guo, X., Kang/'a, S., Kooij, T. W. A., Korsinczky, M., Meyer, E. V. S., Nene, V., Paulsen, I., White, O., Ralph, S. A., Ren, Q., Sargeant, T. J., Salzberg, S. L., Stoeckert, C. J., Sullivan, S. A., Yamamoto, M. M., Hoffman, S. L., Wortman, J. R., Gardner, M. J., Galinski, M. R., Barnwell, J. W., and Fraser-Liggett, C. M. (2008) Comparative genomics of the neglected human malaria parasite Plasmodium vivax, *Nature 455*, 757-763.
7. WHO. (2010) Global report on antimalarial efficacy and drug resistance: 2000-2010, In *WHO 2010*, Geneva.
8. Gardner, M. J., Hall, N., Fung, E., White, O., Berriman, M., Hyman, R. W., Carlton, J. M., Pain, A., Nelson, K. E., Bowman, S., Paulsen, I. T., James, K., Eisen, J. A., Rutherford, K., Salzberg, S. L., Craig, A., Kyes, S., Chan, M.-S., Nene, V., Shallom, S. J., Suh, B., Peterson, J., Angiuoli, S., Pertea, M., Allen, J., Selengut, J., Haft, D., Mather, M. W., Vaidya, A. B., Martin, D. M. A., Fairlamb, A. H., Fraunholz, M. J., Roos, D. S., Ralph, S. A., McFadden, G. I., Cummings, L. M., Subramanian, G. M., Mungall, C., Venter, J. C., Carucci, D. J., Hoffman, S. L., Newbold, C., Davis, R. W., Fraser, C. M., and Barrell, B. (2002) Genome sequence of the human malaria parasite Plasmodium falciparum, *Nature 419*, 498-511.
9. Mathews, V. H., Ahern (2000) *Biochemistry*, Third ed., Addison Wesley Longman, San Francisco.
10. (2008) Protein production and purification, *Nat Meth 5*, 135-146.
11. Studier, F. W., and Moffatt, B. A. (1986) Use of bacteriophage T7 RNA polymerase to direct selective high-level expression of cloned genes, *Journal of Molecular Biology 189*, 113-130.
12. (2010) *Principles and Techniques of Biochemistry and Molecular Biology*, 7th ed., Cambridge University Press, New York.
13. Chayen, N. E., and Saridakis, E. (2008) Protein crystallization: from purified protein to diffraction-quality crystal, *Nat Meth 5*, 147-153.
14. Asherie, N. (2004) Protein crystallization and phase diagrams, *Methods 34*, 266-272.
15. Farrow, R. E., Green, J., Katsimitsoulia, Z., Taylor, W. R., Holder, A. A., and Molloy, J. E. (2011) The mechanism of erythrocyte invasion by the malarial parasite, Plasmodium falciparum, *Seminars in Cell & Developmental Biology 22*, 953-960.

16. Beeson, J. G., and Brown, G. V. (2002) Pathogenesis of Plasmodium falciparum malaria: the roles of parasite adhesion and antigenic variation, *Cellular and Molecular Life Sciences 59*, 258-271.
17. Wirth, D. F. (2002) The parasite genome: Biological revelations, *Nature 419*, 495-496.
18. Stevenson, M. M., and Riley, E. M. (2004) Innate immunity to malaria, *Nat Rev Immunol 4*, 169-180.
19. Thoden, J. B., Phillips, G. N., Neal, T. M., Raushel, F. M., and Holden, H. M. (2001) Molecular Structure of Dihydroorotase: A Paradigm for Catalysis through the Use of a Binuclear Metal Center†,‡, *Biochemistry 40*, 6989-6997.
20. Nørager, S., Jensen, K. F., Björnberg, O., and Larsen, S. (2002) E. coli Dihydroorotate Dehydrogenase Reveals Structural and Functional Distinctions between Different Classes of Dihydroorotate Dehydrogenases, *Structure 10*, 1211-1223.
21. Chen, J.-J., and Jones, M. E. (1976) The cellular location of dihydroorotate dehydrogenase: Relation to de novo biosynthesis of pyrimidines, *Archives of Biochemistry and Biophysics 176*, 82-90.
22. Rawls, J., Knecht, W., Diekert, K., Lill, R., and Löffler, M. (2000) Requirements for the mitochondrial import and localization of dihydroorotate dehydrogenase, *European Journal of Biochemistry 267*, 2079-2087.
23. Nagano, N., Orengo, C. A., and Thornton, J. M. (2002) One Fold with Many Functions: The Evolutionary Relationships between TIM Barrel Families Based on their Sequences, Structures and Functions, *Journal of Molecular Biology 321*, 741-765.
24. Holm, L., and Sander, C. (1997) An evolutionary treasure: unification of a broad set of amidohydrolases related to urease, *Proteins: Structure, Function, and Bioinformatics 28*, 72-82.
25. Benning, M. M., Kuo, J. M., Raushel, F. M., and Holden, H. M. (1994) Three-Dimensional Structure of Phosphotriesterase: An Enzyme Capable of Detoxifying Organophosphate Nerve Agents, *Biochemistry 33*, 15001-15007.
26. Jerapan, K. (1995) Purification, characterization and localization of mitochondrial dihydroorotate dehydrogenase in Plasmodium falciparum, human malaria parasite, *Biochimica et Biophysica Acta (BBA) - General Subjects 1243*, 351-360.
27. Löffler, M., Knecht, W., Rawls, J., Ullrich, A., and Dietz, C. (2002) Drosophila melanogaster dihydroorotate dehydrogenase: the N-terminus is important for biological function in vivo but not for catalytic properties in vitro, *Insect Biochemistry and Molecular Biology 32*, 1159-1169.
28. Painter, H. J., Morrisey, J. M., Mather, M. W., and Vaidya, A. B. (2007) Specific role of mitochondrial electron transport in blood-stage Plasmodium falciparum, *Nature 446*, 88-91.
29. Hansen, M., Le Nours, J., Johansson, E., Antal, T., Ullrich, A., Löffler, M., and Larsen, S. (2004) Inhibitor binding in a class 2 dihydroorotate dehydrogenase causes variations in the membrane-associated N-terminal domain, *Protein Science 13*, 1031-1042.
30. McLean, J. E., Neidhardt, E. A., Grossman, T. H., and Hedstrom, L. (2001) Multiple Inhibitor Analysis of the Brequinar and Leflunomide Binding Sites on Human Dihydroorotate Dehydrogenase†, *Biochemistry 40*, 2194-2200.
31. Phillips, M. A., and Rathod, P. K. (2010) Plasmodium dihydroorotate dehydrogenase: A promising target for novel anti-malarial chemotherapy, *Infectious Disorders - Drug Targets 10*, 226-239.

32. Liu, S., Neidhardt, E. A., Grossman, T. H., Ocain, T., and Clardy, J. (2000) Structures of human dihydroorotate dehydrogenase in complex with antiproliferative agents, *Structure 8*, 25-33.
33. Krungkrai, S. R., Wutipraditkul, N., and Krungkrai, J. (2008) Dihydroorotase of human malarial parasite Plasmodium falciparum differs from host enzyme, *Biochemical and Biophysical Research Communications 366*, 821-826.
34. Deng, X., Gujjar, R., El Mazouni, F., Kaminsky, W., Malmquist, N. A., Goldsmith, E. J., Rathod, P. K., and Phillips, M. A. (2009) Structural plasticity of malaria dihydroorotate dehydrogenase allows selective binding of diverse chemical scaffolds, *Journal of Biological Chemistry 284*, 26999-27009.
35. Hurt, D. E., Widom, J., and Clardy, J. (2006) Structure of Plasmodium falciparum dihydroorotate dehydrogenase with a bound inhibitor, *Acta Crystallographica Section D: Biological Crystallography 62*, 312-323.
36. Booker, M. L., Bastos, C. M., Kramer, M. L., Barker Jr, R. H., Skerlj, R., Sidhu, A. B., Deng, X., Celatka, C., Cortese, J. F., Guerrero Bravo, J. E., Crespo Llado, K. N., Serrano, A. E., Angulo-Barturen, I., Jiménez-Díaz, M. B., Viera, S., Garuti, H., Wittlin, S., Papastogiannidis, P., Lin, J. W., Janse, C. J., Khan, S. M., Duraisingh, M., Coleman, B., Goldsmith, E. J., Phillips, M. A., Munoz, B., Wirth, D. F., Klinger, J. D., Wiegand, R., and Sybertza, E. (2010) Novel inhibitors of Plasmodium falciparum dihydroorotate dehydrogenase with anti-malarial activity in the mouse model, *Journal of Biological Chemistry 285*, 33054-33064.
37. Coteron, J. M., Marco, M., Esquivias, J., Deng, X., White, K. L., White, J., Koltun, M., El Mazouni, F., Kokkonda, S., Katneni, K., Bhamidipati, R., Shackleford, D. M., Angulo-Barturen, I., Ferrer, S. B., Jiménez-Díaz, M. B., Gamo, F. J., Goldsmith, E. J., Charman, W. N., Bathurst, I., Floyd, D., Matthews, D., Burrows, J. N., Rathod, P. K., Charman, S. A., and Phillips, M. A. (2011) Structure-guided lead optimization of triazolopyrimidine-ring substituents identifies potent plasmodium falciparum dihydroorotate dehydrogenase inhibitors with clinical candidate potential, *Journal of Medicinal Chemistry 54*, 5540-5561.
38. Hurt, D. E., Sutton, A. E., and Clardy, J. (2006) Brequinar derivatives and species-specific drug design for dihydroorotate dehydrogenase, *Bioorganic and Medicinal Chemistry Letters 16*, 1610-1615.
39. Malmquist, N. A., Baldwin, J., and Phillips, M. A. (2007) Detergent-dependent kinetics of truncated Plasmodium falciparum dihydroorotate dehydrogenase, *Journal of Biological Chemistry 282*, 12678-12686.
40. Yang, Y., Li, Z., Nan, P., and Zhang, X. (2011) Drug-induced glucose-6-phosphate dehydrogenase deficiency-related hemolysis risk assessment, *Computational Biology and Chemistry 35*, 189-192.
41. Davies, M., Heikkilä, T., McConkey, G. A., Fishwick, C. W. G., Parsons, M. R., and Johnson, A. P. (2009) Structure-Based Design, Synthesis, and Characterization of Inhibitors of Human and Plasmodium falciparum Dihydroorotate Dehydrogenases†, *Journal of Medicinal Chemistry 52*, 2683-2693.
42. Bolanos-Garcia, V. M., and Davies, O. R. (2006) Structural analysis and classification of native proteins from E. coli commonly co-purified by immobilised metal affinity chromatography, *Biochimica et Biophysica Acta (BBA) - General Subjects 1760*, 1304-1313

Appendix A

N-terminal truncated minus loop

Pfa-2b_6xhis

ATGCACCATCATCATCATCATTCTTCTGGTGTAGATCTGGGTACCGAGAAC
CTGTACTTCCAATCCATGTTTGAAAGCTATAATCCGGAATTTTTCCTGTAC
GATATCTTTCTGAAATTTTGCCTGAAATACATCGATGGCGAAATTTGTCAT
GACCTGTTTCTGCTGCTGGGCAAATATAAATTCTGCCGTATGATACCAGCA
ACGATAGCATTTATGCCTGCACCAACATCAAACACCTGGATTTTATTAATC
CGTTTGGTGTTGCAGCCGGTTTTGATAAAAATGGTGTTTGCATTGATAGCA
TCCTGAAACTGGGCTTTAGCTTTATTGAAATTGGCACCATTACACCGCGTG
GTCAGACCGGTAATGCAAAACCGCGTATTTTTCGTGATGTTGAAAGTCGC
TCTATTATTAATAGCTGCGGCTTTAATAACATGGGCTGTGATAAAGTGACC
GAAAACCTGATTCTGTTTCGTAAACGCCAAGAAGAAGATAAACTGCTGAG
CAAACATATTGTGGGTGTTAGCATCGGCAAAAATAAAGATACCGTGAACA
TCGTGGATGACCTGAAATATTGCATCAACAAAATTGGTCGCTATGCCGAT
TATATTGCCATTAATGTTAGCAGCCCGAATACACCGGGTCTGCGTGATAAT
CAAGAAGCAGGTAAACTGAAAAACATTATCCTGAGCGTGAAAGAAGAGA
TCGACAATCTGGAAAAAAACAACATCATGAACGACGAGTTTCTGTGGTTC
AACACCACCAAAAAAAAACCGCTGGTGTTTGTTAAACTGGCACCGGATCT
GAATCAAGAACAGAAAAAAGAAATCGCCGATGTTCTGCTGGAAACCAAT
ATTGATGGCATGATTATTAGCAATACCACCACCCAGATCAACGACATTAA
AAGCTTTGAGAACAAAAAAGGTGGTGTTAGCGGTGCAAAACTGAAAGAT
ATCAGCACCAAATTCATCTGCGAGATGTATAACTACACCAACAAACAAAT
CCCGATTATTGCAAGCGGTGGTATTTTTAGCGGTCTGGATGCACTGGAAA
AAATTGAAGCCGGTGCAAGCGTTTGTCAGCTGTATAGCTGTCTGGTTTTTA
ATGGTATGAAAAGCGCAGTGCAGATTAAACGTGAACTGATCATCTGCTGT
ATCAGCGTGGCTATTATAATCTGAAAGAAGCCATTGGTCGCAAACACAGC
AAAAGCTAA

MHHHHHHSSGVDLGTENLYFQSMFESYNPEFFLYDIFLKFCLKYIDGEICHDL
FLLLGKYNILPYDTSNDSIYACTNIKHLDFINPFGVAAGFDKNGVCIDSILKLG
FSFIEIGTITPRGQTGNAKPRIFRDVESRSIINSCGFNNMGCDKVTENLILFRKR
QEEDKLLSKHIVGVSIGKNKDTVNIVDDLKYCINKIGRYADYIAINVSSPNTPG
LRDNQEAGKLKNIILSVKEEIDNLEKNNIMNDEFLWFNTTKKKPLVFVKLAPD
LNQEQKKEIADVLLETNIDGMIISNTTTQINDIKSFENKKGGVSGAKLKDISTK
FICEMYNYTNKQIPIIASGGIFSGLDALEKIEAGASVCQLYSCLVFNGMKSAVQ
IKRELNHLLYQRGYYNLKEAIGRKHSKS-

Figure 19: N-terminal truncated and minus surface loop Pfa2b_6xhis Construct

```
Alignment of Sequence_1:  [pfa2b_6xhis.xdna] with Sequence_2: [pfa2b_2F_8xhis.xdna]

Similarity: 932/933 (99.89 %)

Seq_1  1     ----------------------------------------ATGCACCATCATCATCATCAT  21
                                                      ||||||||||||||||||||
Seq_2  1     TAGAATAATTTTGTTTAACTTTAAGAAGGAGATATACATATGCACCATCATCATCATCAT  60

Seq_1  22    ------TCTTCTGGTGTAGATCTGGGTACCGAGAACCTGTACTTCCAATCCATGTTTGAA  75
                   ||||||||||||||||||||||||||||||||||||||||||||||||||||||
Seq_2  61    CATCATTCTTCTGGTGTAGATCTGGGTACCGAGAACCTGTACTTCCAATCCATGTTTGAA  120

Seq_1  76    AGCTATAATCCGGAATTTTTCCTGTACGATATCTTTCTGAAATTTTGCCTGAAATACATC  135
             ||||||||||||||||||||||||||||||||||||||||||||||||||||||||||||
Seq_2  121   AGCTATAATCCGGAATTTTTCCTGTACGATATCTTTCTGAAATTTTGCCTGAAATACATC  180

Seq_1  136   GATGGCGAAATTTGTCATGACCTGTTTCTGCTGCTGGGCAAATATAATATTCTGCCGTAT  195
             ||||||||||||||||||||||||||||||||||||||||||||||||||||||||||||
Seq_2  181   GATGGCGAAATTTGTCATGACCTGTTTCTGCTGCTGGGCAAATATAATATTCTGCCGTAT  240

Seq_1  196   GATACCAGCAACGATAGCATTTATGCCTGCACCAACATCAAACACCTGGATTTTATTAAT  255
             ||||||||||||||||||||||||||||||||||||||||||||||||||||||||||||
Seq_2  241   GATACCAGCAACGATAGCATTTATGCCTGCACCAACATCAAACACCTGGATTTTATTAAT  300

Seq_1  256   CCGTTTGGTGTTGCAGCCGGTTTTGATAAAAATGGTGTTTGCATTGATAGCATCCTGAAA  315
             ||||||||||||||||||||||||||||||||||||||||||||||||||||||||||||
Seq_2  301   CCGTTTGGTGTTGCAGCCGGTTTTGATAAAAATGGTGTTTGCATTGATAGCATCCTGAAA  360

Seq_1  316   CTGGGCTTTAGCTTTATTGAAATTGGCACCATTACACCGCGTGGTCAGACCGGTAATGCA  375
             ||||||||||||||||||||||||||||||||||||||||||||||||||||||||||||
Seq_2  361   CTGGGCTTTAGCTTTATTGAAATTGGCACCATTACACCGCGTGGTCAGACCGGTAATGCA  420

Seq_1  376   AAACCGCGTATTTTTCGTGATGTTGAAAGTCGCTCTATTATTAATAGCTGCGGCTTTAAT  435
             ||||||||||||||||||||||||||||||||||||||||||||||||||||||||||||
Seq_2  421   AAACCGCGTATTTTTCGTGATGTTGAAAGTCGCTCTATTATTAATAGCTGCGGCTTTAAT  480

Seq_1  436   AACATGGGCTGTGATAAAGTGACCGAAAACCTGATTCTGTTTCGTAAACGCCAAGAAGAA  495
             ||||||||||||||||||||||||||||||||||||||||||||||||||||||||||||
Seq_2  481   AACATGGGCTGTGATAAAGTGACCGAAAACCTGATTCTGTTTCGTAAACGCCAAGAAGAA  540

Seq_1  496   GATAAACTGCTGAGCAAACATATTGTGGGTGTTAGCATCGGCAAAAATAAAGATACCGTG  555
             ||||||||||||||||||||||||||||||||||||||||||||||||||||||||||||
Seq_2  541   GATAAACTGCTGAGCAAACATATTGTGGGTGTTAGCATCGGCAAAAATAAAGATACCGTG  600

Seq_1  556   AACATCGTGGATGACCTGAAATATTGCATCAACAAAATTGGTCGCTATGCCGATTATATT  615
             ||||||||||||||||||||||||||||||||||||||||||||||||||||||||||||
Seq_2  601   AACATCGTGGATGACCTGAAATATTGCATCAACAAAATTGGTCGCTATGCCGATTATATT  660

Seq_1  616   GCCATTAATGTTAGCAGCCCGAATACACCGGGTCTGCGTGATAATCAAGAAGCAGGTAAA  675
             ||||||||||||||||||||||||||||||||||||||||||||||||||||||||||||
Seq_2  661   GCCATTAATGTTAGCAGCCCGAATACACCGGGTCTGCGTGATAATCAAGAAGCAGGTAAA  720
```

Figure 20: Sequence alignment showing successful Quick-change reaction to make Pfa2b_8xhis Construct; two inserted histidines highlighted in red. (Local alignment done in Serial Cloner 2.1 Software)

N-Terminal truncated minus loop

Pfa2b_8xhis

TAGAATAATTTTGTTTAACTTTAAGAAGGAGATATACATATGCACCATCATCATCAT
CATCATCATTCTTCTGGTGTAGATCTGGGTACCGAGAACCTGTACTTCCAATCCATGT
TTGAAAGCTATAATCCGGAATTTTTCCTGTACGATATCTTTCTGAAATTTTGCCTGAA
ATACATCGATGGCGAAATTTGTCATGACCTGTTTCTGCTGCTGGGCAAATATAATAT
TCTGCCGTATGATACCAGCAACGATAGCATTTATGCCTGCACCAACATCAAACACCT
GGATTTTATTAATCCGTTTGGTGTTGCAGCCGGTTTTGATAAAAATGGTGTTTGCATT
GATAGCATCCTGAAACTGGGCTTTAGCTTTATTGAAATTGGCACCATTACACCGCGT
GGTCAGACCGGTAATGCAAAACCGCGTATTTTTCGTGATGTTGAAAGTCGCTCTATT
ATTAATAGCTGCGGCTTTAATAACATGGGCTGTGATAAAGTGACCGAAAACCTGATT
CTGTTTCGTAAACGCCAAGAAGAAGATAAACTGCTGAGCAAACATATTGTGGGTGTT
AGCATCGGCAAAAATAAAGATACCGTGAACATCGTGGATGACCTGAAATATTGCAT
CAACAAAATTGGTCGCTATGCCGATTATATTGCCATTAATGTTAGCAGCCCGAATAC
ACCGGGTCTGCGTGATAATCAAGAAGCAGGTAAACTGAAAAACATTATCCTGAGCG
TGAAAGAAGAGATCGACAATCTGGAAAAAAACAACATCATGAACGACGAGTTTCTG
TGGTTCAACACCACCAAAAAAAAACCGCTGGTGTTTGTTAAACTGGCACCGGATCTG
AATCAAGAACAGAAAAAAGAAATCGCCGATGTTCTGCTGGAAACCAATATTGATGG
CATGATTATTAGCAATACCACCACCCAGATCAACGACATTAAAAGCTTTGAGAACA
AAAAGGGGGTG

MHHHHHHHHSSGVDLGTENLYFQSMFESYNPEFFLYDIFLKFCLKYIDGEICHDLFLLLG
KYNILPYDTSNDSIYACTNIKHLDFINPFGVAAGFDKNGVCIDSILKLGFSFIEIGTITPRGQ
TGNAKPRIFRDVESRSIINSCGFNNMGCDKVTENLILFRKRQEEDKLLSKHIVGVSIGKNK
DTVNIVDDLKYCINKIGRYADYIAINVSSPNTPGLRDNQEAGKLKNIILSVKEEIDNLEKN
NIMNDEFLWFNTTKKKPLVFVKLAPDLNQEQKKEIADVLLETNIDGMIISNTTTQINDIKS
FENKKGV

Figure 21: N-Terminal truncated and minus surface loop Pfa2b_8xhis Construct

N-terminal truncated and minus surface loop

Pvi-1 construct

caatccATGTTTGAAAGCTATGATCCGGAATTTTTTCTGTATGATGTGTTTCTG
AAAATGCTGCTGAAATATGTGGATGGTGAAACCTGTCATGAACTGTTTCG
CTGATGGGCAAATATAAACTGCTGCCGTATGATACCGGCAAAGATAATAT
TTATAGCTGCAGCGAAATTAAAGGCCTGAATTTTATTAATCCGTTTGGTGT
TGCCGCAGGCTTTGATAAAAATGGTGTTTGCATTGATGGCATTCTGAAACT
GGGCTTTAGCTTTATTGAAATTGGCACCATTACCCCGAAAGATGGTAGCG
ATAAAACCAAACAGCTGGAAGAAGAAATGAAAAAACTGAATGAACAAAT
TGCACAGAAAGGTAATGAACGTCCGCGTATTTTTCGTGATCTGGAAACCC
GTAGCATTATTAATAGCTGCGGCTTTAATAATATGGGCTGTGATGAAGTGT
GCAAAAATCTGAAACGTTTTCGTGAACGCCAGAAAACCGATAAACTGCTG
CAGCGTCATCTGGTTGGTGTGAGCCTGGGTAAAAATAAAGATAGTCCGGA
TATTCTGCAGGATCTGAGCTATTGCATTGGTAAAATTGGTCGCTATGCCGA
TTATATTGCCATTAATGTTAGCAGCCCGAATACACCGGGTCTGCGTGATCA
TCAGAAAGGTGAACGTCTGCATGGTATTATTCAGCGTGTTAAAGAAGAAG
TGGCCAAACTGGACGGTGGTGGTGCACCGCTGGGTGGTGCCACCACAGGT
GGTGCAGCAATGGGTGGCGAACCGTGGGCAAATACCACCAAACGTCGTCC
GCTGATTTTTGTTAAACTGGCACCGGATCTGGAAGAAGGTGAACGTAAAA
GCATTGCAAATGTTCTGCTGAATGCCGAAGTGGATGGTATGATTATTTGTA
ATACCACCACCCAGAAATTTAATATTAAAAGCTTTGAAGATAAAAAAGGT
GGCGTGAGCGGTGAAAAACTGAAAGGTGTTAGCACCCACATGATTAGCCA
GATGTATAATTATACCAATGGCAAAATTCCGATTATTGCCAGCGGTGGTA
TTTTTACCGGTGAAGATGCACTGGAAAAAATTGAAGCCGGTGCAAGCGTT
TGTCAGCTGTATAGCTGTCTGGTTTTTAATGGTATGAAAGCAGCCGTGCGT
ATTAAACGTGAACTGGATCATCTGCTGTATCAGCGTGGTTATTATAAACTG
GGTGATGCAGTTGGTCGTGCACATCGTCGTGCAGCATAA

QSMFESYDPEFFLYDVFLKMLLKYVDGETCHELFLLMGKYKLLPYDTGKDNI
YSCSEIKGLNFINPFGVAAGFDKNGVCIDGILKLGFSFIEIGTITPKDGSDKTKQ
LEEEMKKLNEQIAQKGNERPRIFRDLETRSIINSCGFNNMGCDEVCKNLKRFR
ERQKTDKLLQRHLVGVSLGKNKDSPDILQDLSYCIGKIGRYADYIAINVSSPN
TPGLRDHQKGERLHGIIQRVKEEVAKLDGGGAPLGGATTGGAAMGGEPWAN
TTKRRPLIFVKLAPDLEEGERKSIANVLLNAEVDGMIICNTTTQKFNIKSFEDK
KGGVSGEKLKGVSTHMISQMYNYTNGKIPIIASGGIFTGEDALEKIEAGASVC
QLYSCLVFNGMKAAVRIKRELDHLLYQRGYYKLGDAVGRAHRRAA*

Figure 22: N-terminal and minus surface loop PvDHODH construct

Table 3: Supplementary data showing Mass Spectrometry analysis of SDS PAGE samples from *Pf*DHODH expressed protein after gel filtration step.

Sample	Accession	Description	Score	Coverage	# Proteins	# Unique Peptides	# Peptides	MW [kDa]	calc. pI	Library
1	Q08210	Dihydroorotate dehydrogenase (quinone), mitochondrial OS=Plasmodium falciparum (isolate 3D7) GN=PFF0160c PE=1 SV=1 - [PYRD_PLAF7]	6797.51	28.12	1	24	24	65.5	9.04	P.falciparum
2	Q08210	Dihydroorotate dehydrogenase (quinone), mitochondrial OS=Plasmodium falciparum (isolate 3D7) GN=PFF0160c PE=1 SV=1 - [PYRD_PLAF7]	1727.45	16.17	1	15	15	65.5	9.04	P.falciparum
2	P0AES7	DNA gyrase subunit B OS=Escherichia coli O157:H7 GN=gyrB PE=3 SV=2 - [GYRB_ECO57]	108.75	7.46	1	7	7	89.9	6.06	E.coli

	A2	Sequence	# PSMs	# Proteins	# Protein Groups	Protein Group Accessions	Modifications	ΔCn
	High	LVSEYNATQK	1	1	1	P0AES7		0
	High	VSATGDDAR	1	1	1	P0AES7		0
	High	SNSYDSSSIK	1	1	1	P0AES7		0
	Medium	RGLSIQR	1	1	1	P0AES7		0
	High	DKLVSSEVK	1	1	1	P0AES7		0
	Medium	TLNAYmDK	1	1	1	P0AES7	M6 (Oxidation)	0
	High	LELVIQR	2	1	1	P0AES7		0

	P09373	Formate acetyltransferase 1 OS=Escherichia coli (strain K12) GN=pflB PE=1 SV=2 - [PFLB_ECOLI]	45.69	2.5	1	2	2	85.3	6.01	
3	Q08210	Dihydroorotate dehydrogenase (quinone), mitochondrial OS=Plasmodium falciparum (isolate 3D7) GN=PFF0160c PE=1 SV=1 - [PYRD_PLAF7]	519.19	12.65	1	10	10	65.5	9.04	P.falciparum
3	P17169	Glucosamine--fructose-6-phosphate aminotransferase [isomerizing] OS=Escherichia coli (strain K12) GN=glmS PE=1 SV=4 - [GLMS_ECOLI]	1507.39	15.76	3	12	12	66.9		E.coli

		A2	Sequence	# PSMs	# Proteins	# Protein Groups	Protein Group Accessions	Modifications		
		High	QDIESNLQYDAGDK	1	3	1	P17169			
		High	RQDIESNLQYDAGDK	3	3	1	P17169			
		High	GAYGTVIMDSR	1	3	1	P17169			
		High	GAYGTVImDSR	4	3	1	P17169	M8 (Oxidation)		
		High	IEALAEDFSDK	2	3	1	P17169			
		High	IEQMLSQDK	4	3	1	P17169			
		High	SNIEEVR	12	3	1	P17169			
		High	IEQmLSQDK	7	3	1	P17169	M4 (Oxidation)		

		High	HPDTLLAAR	7	3	1	P17169	
		High	GTDVDQPR	7	3	1	P17169	
		High	HHALFLGR	2	3	1	P17169	
		High	IEQMLSQDKR	6	3	1	P17169	
		High	EIYEQPNAIK	2	3	1	P17169	
		High	IEQmLSQDKR	7	3	1	P17169	M4(Oxidation)
		High	SVNIFDK	4	3	1	P17169	
P64588	Uncharacterized protein yqjI OS=Escherichia coli (strain K12) GN=yqjI PE=4 SV=1 - [YQJI_ECOLI]	103.46	18.36	1	4	4	23.4	
		A2	Sequence	# PSMs	# Proteins	# Protein Groups	Protein Group Accessions	Modifications
		High	VNQSDISDAQIK	1	1	1	P64588	
		High	EQVEmIEER	1	1	1	P64588	M5(Oxidation)
		High	IIAVIDR	1	1	1	P64588	
		High	DDSHGYELIK	1	1	1	P64588	
P0A9W4	Uncharacterized ABC transporter ATP-binding protein YjjK OS=Escherichia coli O157:H7 GN=yjjK PE=3 SV=2 - [YJJK_ECO57]	33.75	3.42	1	2	2	62.4	